

# Enzyme-Specific Coupling of Oxygen and Nitrogen Isotope Fractionation of the Nap and Nar Nitrate Reductases

Ciara K. Asamoto,\* Kaitlin R. Rempfert, Victoria H. Luu, Adam D. Younkin, and Sebastian H. Kopf



Cite This: <https://dx.doi.org/10.1021/acs.est.0c07816>



Read Online

ACCESS |



Metrics & More

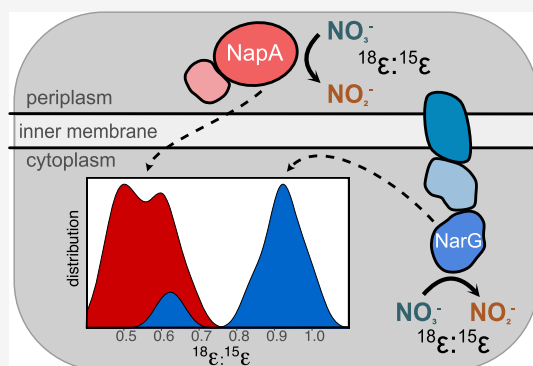


Article Recommendations



Supporting Information

**ABSTRACT:** Dissimilatory nitrate reduction (DNR) to nitrite is the first step in denitrification, the main process through which bioavailable nitrogen is removed from ecosystems. DNR is catalyzed by both cytosolic (Nar) and periplasmic (Nap) nitrate reductases and fractionates the stable isotopes of nitrogen ( $^{14}\text{N}$ ,  $^{15}\text{N}$ ) and oxygen ( $^{16}\text{O}$ ,  $^{18}\text{O}$ ), which is reflected in residual environmental nitrate pools. Data on the relationship between the pattern in oxygen vs nitrogen isotope fractionation ( $^{18}\epsilon/^{15}\epsilon$ ) suggests that systematic differences exist between marine and terrestrial ecosystems that are not fully understood. We examined the  $^{18}\epsilon/^{15}\epsilon$  of nitrate-reducing microorganisms that encode Nar, Nap, or both enzymes, as well as gene deletion mutants of Nar and Nap to test the hypothesis that enzymatic differences alone could explain the environmental observations. We find that the distribution of  $^{18}\epsilon/^{15}\epsilon$  fractionation ratios of all examined nitrate reductases forms two distinct peaks centered around an  $^{18}\epsilon/^{15}\epsilon$  proportionality of 0.55 (Nap) and 0.91 (Nar), with the notable exception of the *Bacillus* Nar reductases, which cluster isotopically with the Nap reductases. Our findings may explain differences in  $^{18}\epsilon/^{15}\epsilon$  fractionation between marine and terrestrial systems and challenge current knowledge about Nar  $^{18}\epsilon/^{15}\epsilon$  signatures.



## INTRODUCTION

Nitrogen is an essential nutrient for life, and consequently, the availability of nitrogen is a vital control on ecosystem productivity. Anthropogenic activity has severely altered the natural balance of the nitrogen cycle. In particular, the use of the Haber–Bosch reaction to synthesize fertilizers has resulted in excess amounts of nitrate and ammonium being introduced into ecosystems.<sup>1,2</sup> Assessing the outcomes of excess nitrogen inputs into ecosystems requires a mechanistic understanding of the competing processes that affect nitrogen cycling in the environment.

Key reductive and oxidative steps in the nitrogen cycle, all of which are catalyzed by microorganisms,<sup>3</sup> are highlighted in Figure 1a. The enzymes bacteria use to reduce or oxidize nitrogen intermediates in the nitrogen cycle impart a kinetic isotope effect on the stable isotopes of nitrogen ( $^{14}\text{N}$ ,  $^{15}\text{N}$ ) and oxygen ( $^{16}\text{O}$ ,  $^{18}\text{O}$ ).<sup>4–9</sup> Because nitrogen fixation by most nitrogenases does not impart strong isotopic fractionation,<sup>9–13</sup> redox cycling of fixed nitrogen, especially the isotopic fractionation associated with dissimilatory nitrate reduction to nitrite, controls the isotopic composition of bioavailable nitrate in many environmental systems. Dissimilatory nitrate reduction is the first step for two processes in the nitrogen cycle, denitrification to  $\text{N}_2$  and dissimilatory nitrate reduction to ammonium (DNRA, also referred to as nitrate ammonification) (Figure 1a). Although these processes serve different

roles, both impact the isotopic composition of residual nitrate in ecosystems through the nitrate reduction step.

The proportionality of N and O isotope fractionation ( $^{18}\epsilon/^{15}\epsilon$ ) associated with nitrate reduction in marine ecosystems generally follows a proportionality of 0.9–1.0.<sup>17–22</sup> In terrestrial ecosystems, observational data with coupled N and O isotope measurements (summarized in Figure 2) suggests that the  $^{18}\epsilon/^{15}\epsilon$  proportionality covers a broader and generally lower range of values between 0.5 and 0.7.<sup>23–29</sup> To date, these systematic differences in  $^{18}\epsilon/^{15}\epsilon$  proportionality are not fully understood and may indicate that we are missing a key feature about how nitrogen cycling processes create the isotopic signatures of nitrate observed in nature. Biogeochemical modeling and recent culturing work suggest that the terrestrial observations of low  $^{18}\epsilon/^{15}\epsilon$  values could be the result of oxidative overprinting of the isotopic signal of nitrate reduction by a combination of nitrate-producing processes such as anaerobic ammonium oxidation (anammox), nitrification, and enzymatic reversibility during

**Received:** November 18, 2020

**Revised:** February 22, 2021

**Accepted:** February 25, 2021



ACS Publications

© XXXX The Authors. Published by  
American Chemical Society

A

<https://dx.doi.org/10.1021/acs.est.0c07816>  
Environ. Sci. Technol. XXXX, XXX, XXX–XXX

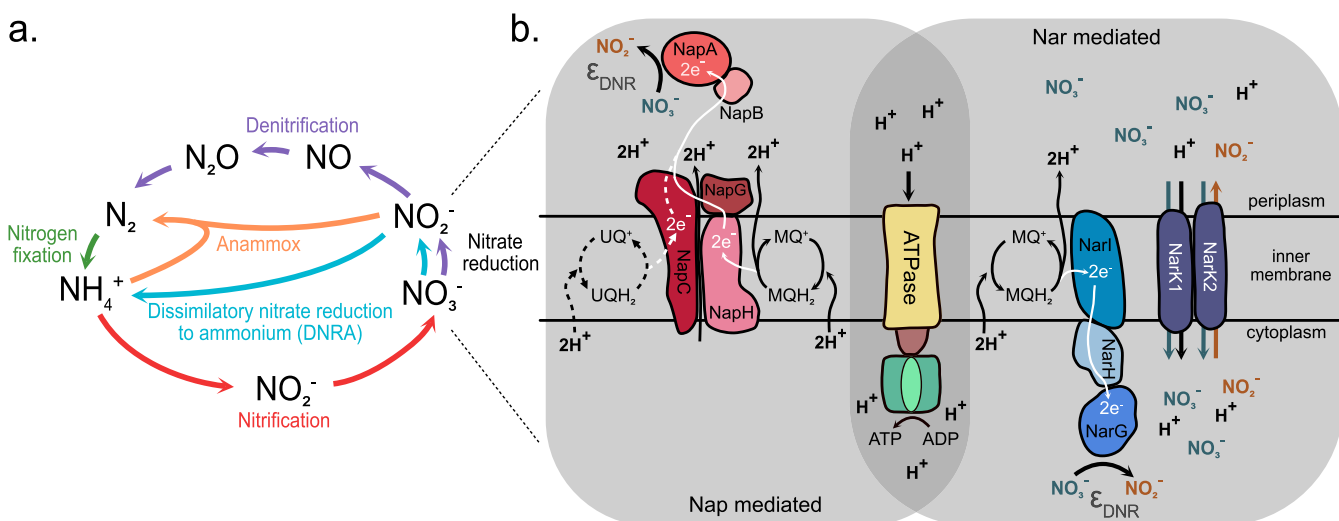


**Figure 1.** (a) Overview of the nitrogen cycle with a focus on the dissimilatory nitrate reduction step. (b) Schematic highlights differences in how nitrate reduction is catalyzed in Nap vs Nar enzymes. Isotope fractionation ( $\epsilon_{\text{DNR}}$ ) occurs during the reduction of nitrate to nitrite. White lines indicate the direction of electron transfer. Black lines indicate proton translocation. In the case of Nap reductases, there are two main potential pathways for nitrate reduction to occur. Bacteria may express NapABC (dashed lines), where NapC oxidizes ubiquinol ( $\text{UQH}_2$ ) to ubiquinone ( $\text{UQ}^+$ ), liberating two protons and two electrons. The electrons are transferred to NapB and then NapA. Alternatively, a bacterium may express NapABCGH (solid lines). Here, NapH oxidizes menaquinol ( $\text{MQH}_2$ ) to menaquinone ( $\text{MQ}^+$ ) and the electrons have an additional transfer step from NapG to NapC, translocating two additional protons.<sup>14,15</sup> The Nar reductase uses NarI to oxidize  $\text{UQH}_2$  to  $\text{UQ}^+$  and transfers electrons to NarH and then NarG.<sup>14,15</sup> NarK1 is a symporter that transports nitrate into the cytoplasm with a proton. NarK2 is an antiporter that couples the import of nitrate to the export of nitrite.<sup>16</sup>

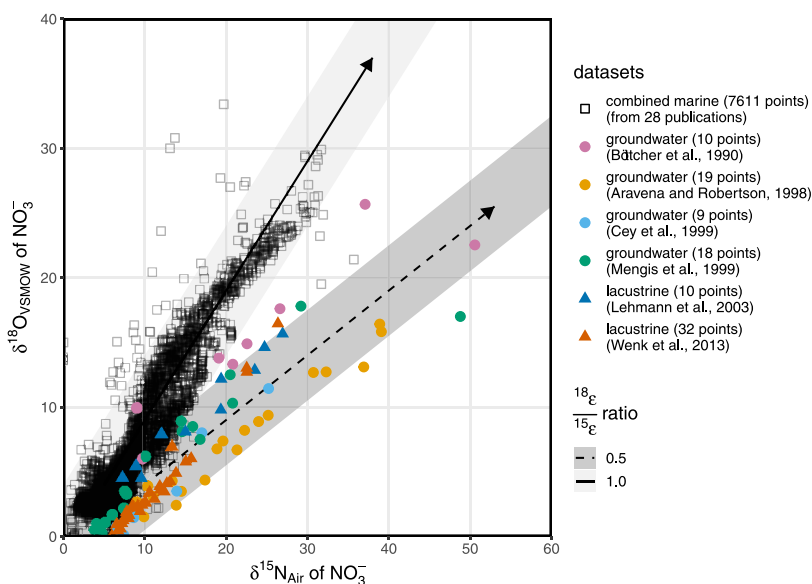


**Figure 2.** Compilation of nitrate isotopic data collected from environmental samples subset into marine and terrestrial/freshwater ecosystems. Solid lines and dashed lines indicate  $^{18}\text{E}/^{15}\text{E}$  proportionalities of 1.0 and 0.5, respectively, with gray-shaded bands showing a range of possible intercepts. See the Supporting Information for details on the literature data.

nitrate reduction.<sup>8,30</sup> However, an alternative hypothesis first proposed by Granger et al.<sup>7</sup> suggests that differences in the  $^{18}\text{E}/^{15}\text{E}$  proportionality observed in nature could actually be a consequence of enzymatic differences during nitrate reduction.

Dissimilatory nitrate reduction can be catalyzed by the periplasmic enzyme Nap (catalytic subunit NapA) and the membrane-bound cytosolic enzyme Nar (catalytic subunit narG). Bacteria can harbor either or both of these nitrate reductases<sup>14,31,32</sup> and neither is linked exclusively to either denitrification or DNRA. The few studies that have specifically examined the isotope effects of Nap reductases<sup>7,33,34</sup> indicate

that Nap N isotope fractionation ( $^{15}\epsilon$ ) ranges from 11.4 to 39.8‰, overlapping with that of Nar reductases (6.6–31.6‰). However, the proportionality between O and N isotope fractionation appears to differ between Nap and Nar-based nitrate reduction. Both the purple photoheterotroph *Rhodospirillum rubrum* and the chemotrophic sulfur oxidizer *Sulfurimonas gotlandica* have only a Nap reductase and were examined by Granger et al.,<sup>7</sup> Treibergs and Granger,<sup>34</sup> and Frey et al.<sup>33</sup> The isotopic data from the Nap reductases in these organisms revealed  $^{18}\text{E}/^{15}\text{E}$  values between 0.57 and 0.68 for *R. rubrum* and 0.43 and 0.68 for *S. gotlandica*, in

contrast with the  $^{18}\text{O}/^{15}\text{N}$  proportionality of  $\sim 0.9$  in Nar-based nitrate reduction.<sup>7,34–36</sup> Here, we present experimental results based on six different nitrate-reducing microorganisms that encode Nar, Nap, or both enzymes, as well as gene deletion mutants of the enzymes' catalytic subunits (NarG and NapA) to test the hypothesis that differences in  $^{18}\text{O}/^{15}\text{N}$  proportionality may stem solely from enzymatic differences and explore the implications of our results for the environmental interpretation of nitrate isotope signatures.

## METHODS

**Strains.** All strains cultured for this study have either the gene for the cytosolic nitrate reductase (narG), the gene for the periplasmic nitrate reductase (napA), or both. The strains that have both narG and napA are *Pseudomonas aeruginosa* PA14 (DSM 19882) and *Paracoccus denitrificans* PD1222, a derivative of DSM 413.<sup>37,38</sup> The strains with only napA are *Desulfovibrio desulfuricans* DSM 642, *Shewanella loihica* DSM (17748),<sup>39–41</sup> and a markerless narG deletion mutant of *P. aeruginosa* PA14,<sup>42</sup> hereafter referred to as PA14  $\Delta$ nar. The strains with only narG are *Bacillus vireti* (DSM 15602), *Bacillus bataviensis* (DSM 15601),<sup>43</sup> and a markerless napA deletion mutant of *P. aeruginosa* PA14, hereafter referred to as PA14  $\Delta$ nap.

**Culturing.** PA14 strains were grown at 30 and 37 °C (PA14  $\Delta$ nar) in defined 3-(N-morpholino)propanesulfonic acid (MOPS) minimal media amended with 25 mM sodium succinate as the sole carbon source,<sup>44</sup> as well as 25 g/L of Luria–Bertani (LB) broth. *B. vireti* and *B. bataviensis* were grown at 30 °C in 30 g/L of tryptic soy broth (TSB) amended with 13 mM glucose and 11 mM sodium succinate.<sup>45</sup> *D. desulfuricans* was grown at 30 °C in Postgate's defined medium,<sup>46</sup> which contains 20 mM lactate and 1 g/L of yeast extract as carbon sources as well as sodium thioglycolate (0.1 g/L) as a reductant. *S. loihica* was grown at 30 °C in a phosphate-buffered minimal salt medium amended with 5, 25, or 30 mM sodium lactate as the sole carbon source (Yoon et al.<sup>47</sup>). *P. denitrificans* was grown at 30 °C in a defined minimal salt medium amended with 25 mM sodium acetate as the sole carbon source (Hahnke et al.<sup>48</sup>). For all nitrate reduction experiments,  $\text{NaNO}_3^-$  was injected from a concentrated stock solution into each culture tube. *S. loihica* media was amended with approximately 10 mM  $\text{NaNO}_3$  in this way, and all other media recipes were amended with approximately 25 mM  $\text{NaNO}_3$ . Exact concentrations in each sample were confirmed by ion chromatography.<sup>47,48</sup>

For all anaerobic growth experiments, media was sparged with  $\text{N}_2$  gas and cultures were incubated while shaking at 250 rpm in balch tubes containing 20 mL of media and 5 mL of  $\text{N}_2$  headspace at 1.1 bar and sealed with blue butyl rubber stoppers. Due to *P. aeruginosa*'s regulation of napA, aerobic conditions were required for the PA14  $\Delta$ nar strain to reduce nitrate (see Results and Discussion for details). For these cultures, culture tubes were incubated while shaking at 250 rpm. Agar plates for reviving strains from frozen stock were prepared by amending each media recipe with 15 g/L of agar. All strains except *D. desulfuricans* (an obligate anaerobe) were revived on aerobic agar plates and passaged three times in liquid medium before inoculating isotope fractionation experiments with 1% culture (v/v). *D. desulfuricans* was inoculated directly from freezer stocks into anaerobic culture medium and passaged five times before inoculating isotope fractionation experiments.

**Isotope Fractionation Experiments.** All strains were grown in triplicate in their respective media in the presence of nitrate and sampled at regular intervals for nitrate consumption and nitrate isotopic composition. Growth was monitored directly in the culture tubes by optical density (OD) using a Spectronic 20 spectrophotometer at a wavelength of 660 nm for *B. vireti* and *B. bataviensis* and 600 nm for all other strains. At each time point, approximately 2 mL of sample was withdrawn through the stopper using a 23-gauge needle attached to a syringe. Syringes were flushed with nitrogen prior to sampling to preserve the anaerobic environment within the balch tubes. Samples were filter-sterilized with 0.2  $\mu\text{m}$  poly(ethersulfone) (PES) filters, aliquoted for later quantification and isotopic analysis, and stored at  $-20$  °C. Aliquots for ion chromatography (IC) were immediately diluted in 0.1 M NaOH (pH 11) to stabilize nitrite. For *P. aeruginosa* and *B. vireti*, the experiment was additionally repeated in media made from  $^{18}\text{O}$  enriched water (OLM-240-10-1, Cambridge Isotope Laboratories, Inc.) at a final  $\delta^{18}\text{O}_{\text{water}}$  of approximately +100‰.

**Sample Analysis.** Nitrate and nitrite concentrations were quantified using a Dionex ICS-6000 Ion Chromatograph equipped with an IonPac AS11-HC column and a variable wavelength absorbance (UV/vis) detector to allow for accurate analyte detection in complex media (LB, TSB). Samples were eluted isocratically with 20 mM KOH at a flow rate of 1 mL/min. Nitrate and nitrite peaks were measured at a wavelength of 210 nm and quantified against laboratory standards prepared in the same media backgrounds. The N and O isotopic compositions of nitrate were determined in the Sigman Lab at Princeton University using the denitrifier method<sup>49,50</sup> with 20 nmol nitrate per analysis. Nitrite removal was performed prior to isotopic analysis for all samples with nitrite concentrations >1% nitrate using the sulfamic acid method.<sup>51</sup> The isotopic measurements were calibrated against the potassium nitrate reference standards IAEA-NO3 ( $\delta^{15}\text{N} = 4.7\text{‰}$  vs air,  $\delta^{18}\text{O} = 25.6\text{‰}$  vs Vienna Standard Mean Ocean Water (VSMOW)), provided by the International Atomic Energy Agency and USGS34 ( $\delta^{15}\text{N} = -1.8\text{‰}$  vs air,  $\delta^{18}\text{O} = -27.9\text{‰}$  vs VSMOW) provided by the United States Geological Survey, each measured at two different concentrations every eight samples to correct for injection volumes. Analytical runs were corrected for instrument drift based on a  $\text{N}_2\text{O}$  drift monitoring standard. All isotopic data are reported in conventional delta notation vs the international reference scales for N (Air) and O (VSMOW):  $\delta^{15}\text{N} = ([^{15}\text{N}/^{14}\text{N}]_{\text{sample}}/[^{15}\text{N}/^{14}\text{N}]_{\text{air}} - 1)$  and  $\delta^{18}\text{O} = ([^{18}\text{O}/^{16}\text{O}]_{\text{sample}}/[^{18}\text{O}/^{16}\text{O}]_{\text{VSMOW}} - 1)$ .  $\delta$  values reported in per mil (‰) are implicitly multiplied by a factor of 1000.<sup>52</sup> The analytical precision of the nitrate monitoring standard used across all analytical runs was 0.06‰ for  $\delta^{15}\text{N}$  and 0.69‰ for  $\delta^{18}\text{O}$  ( $1\sigma$ ,  $n = 33$ ). Additionally, all fractionation experiments were run using the same nitrate source in different media; thus, initial time points across all experiments provide an estimate of the sample analytical precision: 0.07‰ for  $\delta^{15}\text{N}$  and 0.43‰ for  $\delta^{18}\text{O}$  ( $1\sigma$ ,  $n = 52$ ).

**Calculations.** All data (in Excel format) and source code (in R Markdown format) used to produce the figures, data tables, and analyses for this paper are available online at [www.github.com/Kopflab/2021\\_Asamoto\\_et\\_al](https://github.com/Kopflab/2021_Asamoto_et_al).

**Isotope Effects.** The nitrate  $\delta^{15}\text{N}$  and  $\delta^{18}\text{O}$  measurements were fit to the following linear equations to estimate the N and O isotope effects ( $^{15}\epsilon$  and  $^{18}\epsilon$ ) and isotope effect

proportionality ( $^{18}\epsilon/^{15}\epsilon$ ) imparted on nitrate during microbial nitrate reduction from the slope of the regressions<sup>53</sup>

$$\ln\left(\frac{\delta^{15}\text{N} + 1}{\delta^{15}\text{N}_{\text{initial}} + 1}\right) = ^{15}\epsilon \cdot \ln(f) \quad (1)$$

$$\ln\left(\frac{\delta^{18}\text{O} + 1}{\delta^{18}\text{O}_{\text{initial}} + 1}\right) = ^{18}\epsilon \cdot \ln(f) \quad (2)$$

$$\ln\left(\frac{\delta^{18}\text{O} + 1}{\delta^{18}\text{O}_{\text{initial}} + 1}\right) = \frac{^{18}\epsilon}{^{15}\epsilon} \cdot \ln\left(\frac{\delta^{15}\text{N} + 1}{\delta^{15}\text{N}_{\text{initial}} + 1}\right) \quad (3)$$

where  $f = [\text{NO}_3^-]/[\text{NO}_3^-]_{\text{initial}}$  is the fraction of nitrate remaining and  $\delta$  and  $\epsilon$  values in per mil (‰) are implicitly multiplied by a factor of 1000.<sup>52</sup> The errors of the regression slopes were used to estimate standard errors for  $^{15}\epsilon$  (eq 1),  $^{18}\epsilon$  (eq 2), and  $^{18}\epsilon/^{15}\epsilon$  (eq 3). Note that for this implementation of the Rayleigh distillation model (eqs 1 and 2), normal kinetic isotope effects (reflecting higher reaction rates of the lighter isotopes) are negative ( $\epsilon < 0$ ) and are reported as such in Table S1. The opposite convention with normal kinetic isotope effects reported as  $\epsilon > 0$  is also not uncommon, and all comparisons with literature data carefully consider the convention used in each publication. For visual representation of eq 3 in figures, the following more intuitive but slightly less accurate linearizations were used (eqs 4–6)

$$\ln\left(\frac{\delta^{15}\text{N} + 1}{\delta^{15}\text{N}_{\text{initial}} + 1}\right) \approx \delta^{15}\text{N} - \delta^{15}\text{N}_{\text{initial}} = \Delta\delta^{15}\text{N} \quad (4)$$

$$\ln\left(\frac{\delta^{18}\text{O} + 1}{\delta^{18}\text{O}_{\text{initial}} + 1}\right) \approx \delta^{18}\text{O} - \delta^{18}\text{O}_{\text{initial}} = \Delta\delta^{18}\text{O} \quad (5)$$

$$\Delta\delta^{18}\text{O} = \frac{^{18}\epsilon}{^{15}\epsilon} \cdot \Delta\delta^{15}\text{N} \quad (6)$$

**Sequence Alignment and Gene Trees.** Amino acid sequences for napA and narG reductase genes (see Table S2 for details) were aligned using the ClustalOmega Multiple Sequence Alignment.<sup>54</sup> A list of gene accession numbers is available in Table S2. Maximum clade credibility gene trees were constructed using the MrBayes' Markov chain Monte Carlo analysis under an inverse  $\gamma$  rate variation model with default parameters.<sup>55</sup>

## RESULTS AND DISCUSSION

**Growth of Cultures.** Growth rates are recorded in Table S1. All growth curves and nitrate consumption data are depicted in Figures S1 and S2. No quantitative growth curve data was collected for *S. loihica* and *D. desulfuricans*. While turbidity was detected in *S. loihica*, clumping prevented accurate optical density measurements. *D. desulfuricans* was grown in Postgate's medium, which precipitates iron sulfides and iron hydroxides, preventing accurate optical density measurements. All strains consumed nitrate successfully under fully anaerobic conditions, except for PA14  $\Delta$ nar, which required  $\text{O}_2$  for growth and only consumed significant quantities of nitrate while also exposed to air. Nitrate consumption differed by strain and medium and ranged from as fast as  $\sim 15$  mM nitrate in 8 h (*B. vireti*) to as slow as 15 mM nitrate in 80 h (PA  $\Delta$ nap). See Figure S2 for details.

Growth in strains of denitrifying bacteria that cannot perform DNRA (*P. aeruginosa*, *P. denitrificans*) (Figure 1) had little to no nitrite accumulation. However, strains of bacteria that have the potential to perform DNRA in addition to denitrification (*B. vireti*, *B. bataviensis*, *D. desulfuricans*, *S. loihica*) concentrated nitrite during the experiments (Figure S2). This was particularly pronounced in *B. vireti* and *B. bataviensis*. Consequently, later time points for these experiments could not be analyzed directly for their nitrate isotopic composition because the sulfamic acid nitrite removal method is only effective to a 7:1 nitrite/nitrate (mol/mol) mixing ratio.<sup>51</sup> Nitrate in several of these samples with exceedingly high nitrite/nitrate ratios was thus separated from nitrite by ion chromatography coupled to fraction collection to enable isotopic measurements. The analytical impact of residual nitrite from incomplete nitrite removal by sulfamic acid is discussed in more detail in the Supporting Information.

During all time course experiments, decreases in nitrate concentration corresponded to an increasingly enriched residual nitrate pool (Figures S3 and S4). Experimental conditions and  $^{18}\epsilon/^{15}\epsilon$  proportionality values are summarized in Table 1.  $^{15}\epsilon$  values ranged from 10.8 to 34.8‰.  $^{18}\epsilon$  values

**Table 1. Summary of Isotope Fractionation Experiments<sup>a</sup>**

organism	reductase gene(s)	medium	$^{18}\epsilon/^{15}\epsilon \pm \text{SE}$
<i>P. aeruginosa</i> PA14	both	LB	$0.97 \pm 0.02$
<i>P. aeruginosa</i> PA14	both	MOPS	$0.63 \pm 0.02$
<i>P. aeruginosa</i> $\Delta$ napA	narG	LB	$0.91 \pm 0.01$
<i>P. aeruginosa</i> $\Delta$ napA	narG	MOPS	$0.85 \pm 0.02$
<i>P. aeruginosa</i> $\Delta$ narG*	napA	LB	$0.49 \pm 0.00$
<i>P. denitrificans</i>	both	Hahnke	$0.92 \pm 0.01$
<i>B. bataviensis</i>	narG	TSB	$0.61 \pm 0.06$
<i>B. vireti</i>	narG	TSB	$0.64 \pm 0.04$
<i>D. desulfuricans</i>	napA	Postgate	$0.63 \pm 0.06$
<i>S. loihica</i>	napA	SL	$0.55 \pm 0.01$

<sup>a</sup>Tracer experiments are included as replicates. Standard error is calculated from all experimental replicates. Asterisk (\*) indicates the strain that required  $\text{O}_2$  for nitrate reduction and was thus grown aerobically.

ranged from 5.2 to 29.6‰ (Table S1). Isotopic data fit a closed-system Rayleigh model for isotope fractionation, with data largely conforming to a linear relationship of  $\delta^{15}\text{N}$  or  $\delta^{18}\text{O}$  vs the natural logarithm of the remaining nitrate (Figures S3 and S4).

**Nitrate Reductases Have Enzyme-Specific  $^{18}\epsilon/^{15}\epsilon$  Coupling.** Our data indicate an enzyme-specific isotope effect for the Nar and Nap reductases. The PA14 knockout nitrate reduction experiments show that the Nap reductase in this organism has an  $^{18}\epsilon/^{15}\epsilon$  proportionality of 0.49, while that of the Nar reductase in the same organism has a value of 0.86–0.91 (Table 1 and Figure 3). The  $^{18}\text{O}$  tracer experiments confirm that no back-reaction of nitrite or exchange with ambient water occurred (Figure S6). The PA14  $\Delta$ nar data was substantiated by the *D. desulfuricans* and *S. loihica* experiments, with  $^{18}\epsilon/^{15}\epsilon$  values of  $0.63 \pm 0.06$  and  $0.55 \pm 0.01$ , respectively (Table 1 and Figure 4). Together, our data suggest that  $^{18}\epsilon/^{15}\epsilon$  differences can be purely enzymatic, challenging the hypothesis that environmental  $^{18}\epsilon/^{15}\epsilon$  patterns require nitrite reoxidation from enzymatic reversibility, nitrification, or anammox.<sup>30</sup> These observations for  $^{18}\epsilon/^{15}\epsilon$  from nitrate reduction by the Nap reductase in PA14  $\Delta$ nar are similar to all other available

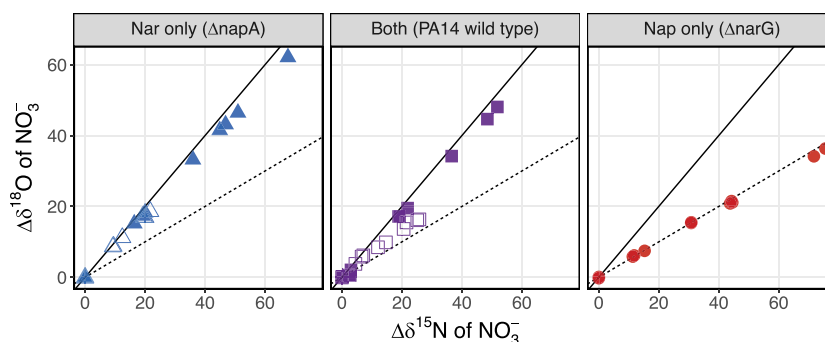


**Figure 3.** Change in  $\delta^{18}\text{O}$  plotted vs change in  $\delta^{15}\text{N}$  for the *P. aeruginosa* PA14 wild type (WT) and mutant experiments. “Nar only” corresponds to the PA14  $\Delta\text{napA}$  strain, and “Nap only” corresponds to the PA14  $\Delta\text{narG}$  strain. Solid lines and dashed lines indicate  $^{18}\epsilon/^{15}\epsilon$  proportionalities of 1.0 and 0.5, respectively. Open points indicate cultures grown in MOPS and filled points indicate cultures grown in LB.

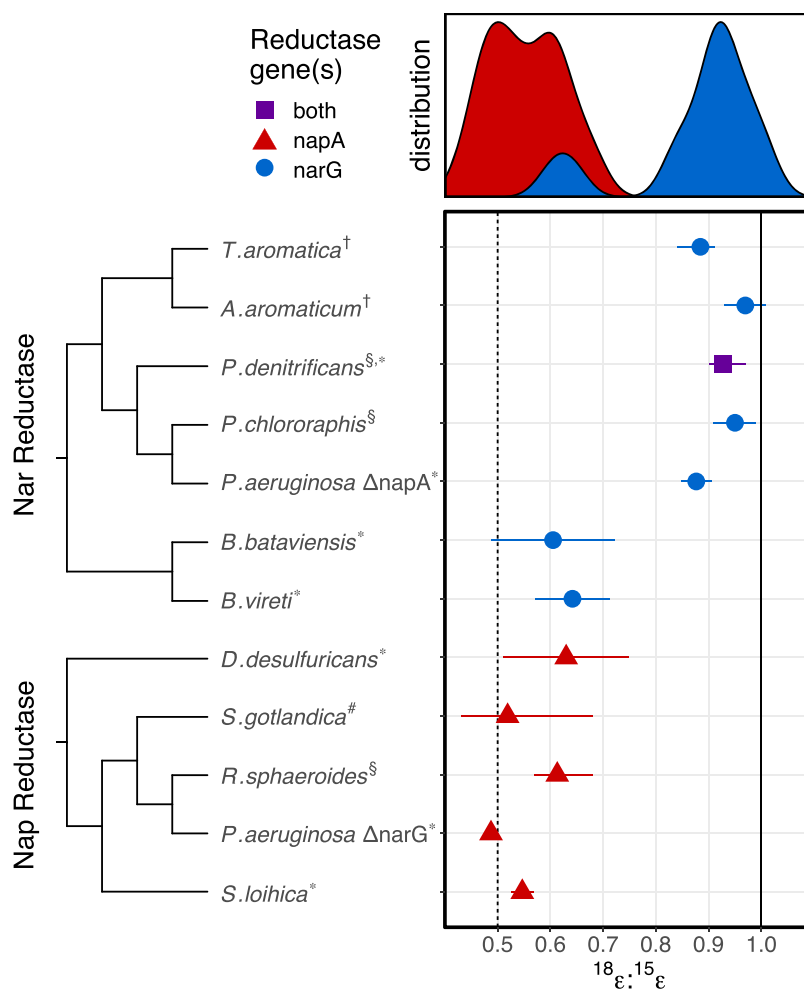


**Figure 4.** Maximum clade credibility gene trees of the Nap and Nar reductases and a summary of known  $^{18}\epsilon/^{15}\epsilon$  values (symbols denote averages, error bars denote value ranges if multiple values available or  $\pm 2$  standard errors for single values) with a distribution of these ranges shown above. Solid line and dashed line indicate  $^{18}\epsilon/^{15}\epsilon$  of 1.0 and 0.5, respectively. Colors and shapes indicate the nitrate reductase that is part of the genome of each strain (blue circles: narG only; red triangles: napA only). *P. denitrificans* (purple square) has both genes but under the culturing conditions employed only uses narG.<sup>59,60</sup> *Escherichia coli* TMAO reductase used as an outgroup in both gene trees. Data collected in this study indicated with an asterisk (\*). Literature data collected from (Frey et al.<sup>33</sup> (#); Granger et al.<sup>7</sup> (§); Wunderlich et al.<sup>36</sup> (†)).

observations from organisms that naturally have only this reductase, with  $^{18}\epsilon/^{15}\epsilon$  couplings of 0.63 and 0.51 observed in *R. sphaeroides* and *S. gotlandica*, respectively<sup>7,33,34</sup> (Figure 4).

As discussed above, the PA14  $\Delta\text{nap}$  strain had an  $^{18}\epsilon/^{15}\epsilon$  proportionality of  $\sim 0.9$ , which is consistent with previous reports from organisms that harbor only Nar (Figure

4).<sup>7,34–36,56</sup> Despite having both nitrate reductases present, *P. denitrificans* has been shown in the literature and in our own experiments to also have an  $^{18}\epsilon/^{15}\epsilon$  coupling of  $0.92 \pm 0.01$ <sup>7,34,35</sup> (Figure 4). Previous research has demonstrated that *P. denitrificans* PD1222 only uses the Nap reductase under microaerobic conditions and/or in the presence of highly

reduced carbon sources.<sup>57,58</sup> The culture conditions for *P. denitrificans* used in this study (completely anaerobic conditions, relatively oxidized carbon sources) are not conducive to Nap expression based on the literature data. The  $^{18}\text{E}/^{15}\text{E}$  signal we observed in our data is therefore consistent with *P. denitrificans* only reducing nitrate with Nar.

In contrast to all other data on Nar reductases, *B. vireti* and *B. bataviensis* have a significantly lower  $^{18}\text{E}/^{15}\text{E}$ :  $0.64 \pm 0.04$  and  $0.61 \pm 0.06$ , respectively (Table 1 and Figure 4). Although  $^{18}\text{E}/^{15}\text{E}$  values between biological replicates covered a wider range than in other organisms, *Bacillus*  $^{18}\text{E}/^{15}\text{E}$  values were consistently lower than all other Nar reductases (Figure 4). Some of the variations could stem from incomplete nitrite removal, nitrite–water exchange, or nitrite back-reaction, but the  $^{18}\text{O}$  tracer experiments suggest that this is not the case and the nitrate isotopic composition for the most nitrite-replete samples was confirmed by the preparative purification of nitrate using ion chromatography (see the Supporting Information for a complete discussion). We also considered growth rate effects as a potential source of these isotopic differences as nitrate reduction rates are known to change the magnitude of fractionation. However, previous work suggests that the  $^{18}\text{E}/^{15}\text{E}$  coupling is preserved even when fractionation factors vary.<sup>35,61</sup> For example, Granger et al.<sup>7</sup> report a wide range of  $^{15}\text{E}$  values (17.6–26.6‰) for *P. denitrificans* yet observe a consistent  $^{18}\text{E}/^{15}\text{E}$  proportionality between 0.90 and 0.95. Even at overlapping growth rates (Table S1), the *B. bataviensis* and *P. denitrificans* cultures maintained distinct  $^{18}\text{E}/^{15}\text{E}$  proportionalities, further suggesting that this is not a growth rate effect. It is also notable that these are the first observations from Gram-positive nitrate reducers. However, unlike in some Archaea,<sup>62</sup> the active site of *Bacillus* NarG is located in the cytoplasm just like their Gram-negative counterparts,<sup>63</sup> which suggests that nitrate reduction takes place in the same biochemical environment. Overall, the *Bacillus* data indicate that it is possible for some Nar reductases to have distinct and lower  $^{18}\text{E}/^{15}\text{E}$  proportionality, adding to the complexity of interpreting isotopic signals of nitrate reduction in ecosystems.

**Roles of Nap and Nar Reductases.** The Nar reductase is known as the primary respiratory reductase among denitrifying bacteria. The nar operon is highly conserved, with narGHI present in every known Nar-bearing denitrifier.<sup>14</sup> Its singular role is in providing energy conservation under anaerobic conditions where high levels of nitrate are present. The Nap reductase, however, has been implicated in both aerobic and traditional anaerobic denitrification, DNRA, redox balancing, nitrate scavenging, and even magnetite biomineralization.<sup>57,58,64–68</sup> The nap operon is much less conserved, with several combinations of the 11 different genes found across species.<sup>14,15,32,69</sup> The regulation of these enzymes also differs. As Nar is distinctly used for respiration, the nar operon is upregulated under anaerobic conditions and by the presence of nitrate. Nap regulation, however, is more complex given the variable operon conformations and assorted functions across species the Nap reductase can perform. For example, reduced carbon sources can upregulate nap expression in some Nap-bearing bacteria.<sup>57,58,60,70</sup> Additionally, the presence of either oxygen or nitrate can up- or downregulate nap expression depending on species.<sup>68,71–73</sup> The gene regulation of these enzymes thus ties the bacterial preference of reducing nitrate with Nar vs Nap to environmental constraints.

Bacterial preference of using the Nar or Nap reductase was exemplified in the wild-type PA14 strain experiments when grown in different media. The wild-type PA14 strain grown in the MOPS medium had an  $^{18}\text{E}/^{15}\text{E}$  proportionality of  $0.63 \pm 0.02$  (Table 1 and Figure 3). This is a midpoint value in comparison to the  $^{18}\text{E}/^{15}\text{E}$  proportionality measured in the PA14  $\Delta\text{nap}$  and PA14  $\Delta\text{nar}$  strains and suggests that PA14 was using both nitrate reductases. The Nap reductase for *P. aeruginosa* is used as a backup redox-balancing mechanism, in particular, under conditions where electron acceptors are limiting.<sup>74</sup> When grown in LB, this strain exhibited a higher  $^{18}\text{E}/^{15}\text{E}$  proportionality of  $0.97 \pm 0.02$  (Table 1). While LB broth is considered a rich medium, it is actually carbon-limited, with mostly amino acids available for uptake.<sup>75</sup> This would cause lower C/N ratios in contrast to the MOPS minimal medium, in which we provide excess succinate as a carbon source. Past research in *E. coli* has shown that the Nar reductase has a selective advantage under low carbon and high nitrate concentrations, which is the case in our LB-grown cultures.<sup>67</sup> Furthermore, this effect does not occur in the PA14  $\Delta\text{nap}$  strain, suggesting that this is not a difference in how the Nar reductase performs in LB vs minimal medium, but a change in the expression pattern by PA14 to maximize energy conservation.

**Mechanism for Isotopic Differences.** Regardless of differences in gene regulation, the Nap and Nar reductases still catalyze the same reaction and yet have different isotope effects. The active sites of both reductases are similar, with both containing a Mo-bis-MGD cofactor and iron sulfur cluster.<sup>14,76</sup> One distinction is that the Nar reductase's Mo center is coordinated by an aspartate residue, while the Nap reductase is coordinated by a cysteine. Cysteine is a more reduced residue that may impact the redox potential of the Mo center, affecting how nitrate is bound and reduced.<sup>77–79</sup> Studies indicate that Nap generally has a higher affinity for nitrate than Nar.<sup>67,80–82</sup> Furthermore, the base of its substrate channel is lined with positively charged amino acid residues that guides nitrate to the active site.<sup>78,83</sup> In contrast, Nar has a substrate channel with negatively charged residues that may impact the rate of nitrate binding overall.<sup>84</sup> Thus, it is possible that the root of isotopic differences lies within the nitrate molecule's interaction with the active site of these enzymes.

Additionally, it has been proposed that nitrate binds to the catalytic site of Nap and Nar differently. For the Nar reductase, the general mechanism for nitrate binding allows nitrate to bind either Mo(V) or Mo(IV), such that an internal electron transfer may be required before the nitrate molecule can be reduced by Nar.<sup>85,86</sup> This is in contrast to the Nap reductase where nitrate binds molybdenum only in the reduced state, Mo(IV), and reduces the nitrate immediately.<sup>69,78</sup> Frey et al.<sup>33</sup> suggested that this may cause a difference in isotope fractionation as the Nar reductase may be subject to an intramolecular isotope effect. While the precise mechanism of nitrate binding and reduction for both Nap and Nar is still uncertain, the Nap reductase's high affinity for nitrate and its faster reduction mechanism may be key in understanding the differences in  $^{18}\text{E}/^{15}\text{E}$  proportionality. Contrary to expectations, our results for the *Bacillus* experiments indicate that a Nap-like isotopic signature with respect to  $^{18}\text{E}/^{15}\text{E}$  proportionality is possible in a Nar reductase. Future work on the structural differences between the *Bacillus* and other Nar reductases may hold the key to uncovering the mechanistic basis for these isotopic differences.

### Interpreting $^{18}\text{E}/^{15}\text{E}$ Proportionality in Ecosystems.

Our research shows that nitrate reduction by Nap reductases consistently produces  $^{18}\text{E}/^{15}\text{E}$  proportionality values that are lower than those observed in marine ecosystems and may explain the  $^{18}\text{E}/^{15}\text{E}$  signals observed in terrestrial ecosystems. The isotopic data sets collected for the terrestrial data in Figure 2 come from a diverse set of ecosystems ranging from soils to lakes to riparian zones and groundwater runoff from agriculture (see the Supporting Information for details). Soils, in particular, can have a large range of redox gradients contained within a few centimeters and experience drastic changes in moisture on short time scales, impacting oxygen availability.<sup>87</sup>

In comparison, marine systems operate at larger scales and experience less heterogeneity over short spatial and temporal scales with dissimilatory nitrate reduction occurring predominantly in oxygen minimum zones (OMZs) and anoxic sediments.<sup>17–20,22</sup> The nar operon has a much narrower regulatory range of permissible environmental conditions than the nap operon and, unlike the latter, is always inhibited by the presence of  $\text{O}_2$  above suboxic ( $10\ \mu\text{M}$ ) concentrations,<sup>88–90</sup> which may explain the predominance of nar-based nitrate reduction in stable low oxygen systems like OMZs.<sup>91,92</sup> It is thus conceivable that the Nap reductase's multiple functions are more suitable for maintaining bacterial homeostasis in terrestrial aquatic ecosystems that can fluctuate significantly over short spatial and temporal time scales.

Though this hypothesis may appear at odds with the established assumption that the Nap reductase is used less commonly than the Nar reductase, limited data is available on Nap vs Nar use in nature. Work by Bru et al.<sup>93</sup> and Smith et al.<sup>94</sup> indicates that Nap and Nar gene copy numbers are roughly equivalent throughout various terrestrial and freshwater environments. Further, slurry incubation experiments performed by Dong et al.<sup>95</sup> indicated that the Nap reductase was more commonly used in one of the three communities of denitrifiers surveyed. While similar studies specifically targeting Nap and Nar gene abundances have not been carried out in marine ecosystems, at minimum, this data indicates that the Nap reductase serves an important role in nitrate reduction for bacteria and that its expression is comparable to Nar in freshwater and terrestrial ecosystems. Additionally, *Bacillus* are common denitrifying bacteria in terrestrial soils.<sup>96</sup> Given their distinctly low  $^{18}\text{E}/^{15}\text{E}$  proportionalities, they may be another significant source of the low  $^{18}\text{E}/^{15}\text{E}$  values observed in terrestrial ecosystems.

Since the Nap reductase is not embedded in the cytosolic membrane and thus not directly involved in proton motive force (PMF) generation, it is frequently presumed to be rarely used for respiration. This explains the common assumption that the isotopic signal of nitrate reduction in ecosystems must stem mainly from the membrane-bound cytosolic Nar reductase, as PMF generation is essential for survival and growth.<sup>7,17,20,34,35</sup> However, the potential to perform nitrate reduction with only a Nap reductase appears to be commonplace, and with the right auxiliary genes present in the nap operon, it can be just as efficient as the Nar reductase at producing a proton motive force (PMF) (Figure 1b).<sup>64,69,97</sup> Future work combining isotopic measurements with quantification of gene expression patterns of the Nap and Nar reductases in different environments can connect our culture-based results back to the trends originally observed in nature. This will be critical when considering the potential impact and extent of *Bacillus*-like Nar enzymes in nature that may have

lower  $^{18}\text{E}/^{15}\text{E}$  values. The regulation patterns observed in the PA14 wild-type strain in MOPS vs LB medium also emphasize the importance of performing transcriptomics and/or proteomics over metagenomics, as bacteria with both reductases may switch between Nap and Nar depending on environmental constraints. This is particularly important when considering processes such as DNRA, which can use either NapA or NarG to reduce nitrate. Though the Nap reductase is often implicated as the main reductase used during DNRA, many species of bacteria appear to catalyze DNRA solely via the Nar reductase.<sup>45,63,98,99</sup> The data presented in this study provides a clear indication that even closely related enzymes can have very distinct isotopic signatures that may allow more comprehensive interpretations of environmental data in the future.

## ■ ASSOCIATED CONTENT

### Supporting Information

The Supporting Information is available free of charge at <https://pubs.acs.org/doi/10.1021/acs.est.0c07816>.

Data summary (Table S1); gene accession numbers (Table S2), growth curves (Figure S1); nitrate and nitrite concentrations vs time (Figure S2);  $\delta^{15}\text{N}$  vs  $\ln f$  (Figure S3);  $\delta^{18}\text{O}$  vs  $\ln f$  (Figure S4);  $\delta^{18}\text{O}$  vs  $\delta^{15}\text{N}$  (Figure S5);  $^{18}\text{O}$  water experiments (Figure S6), and supplemental discussion on impacts of nitrite accumulation and information about data collection for Figure 1 (PDF)

## ■ AUTHOR INFORMATION

### Corresponding Author

Ciara K. Asamoto – Department of Geological Sciences, University of Colorado Boulder, Boulder, Colorado 80309, United States; [orcid.org/0000-0003-0981-3190](https://orcid.org/0000-0003-0981-3190); Email: [ciara.asamoto@colorado.edu](mailto:ciara.asamoto@colorado.edu)

### Authors

Kaitlin R. Rempfert – Department of Geological Sciences, University of Colorado Boulder, Boulder, Colorado 80309, United States

Victoria H. Luu – Department of Geosciences, Princeton University, Princeton, New Jersey 08544, United States

Adam D. Younkin – Department of Geological Sciences, University of Colorado Boulder, Boulder, Colorado 80309, United States

Sebastian H. Kopf – Department of Geological Sciences, University of Colorado Boulder, Boulder, Colorado 80309, United States

Complete contact information is available at: <https://pubs.acs.org/doi/10.1021/acs.est.0c07816>

### Notes

The authors declare no competing financial interest.

## ■ ACKNOWLEDGMENTS

This research was supported by the Department of Geological Sciences at the University of Colorado Boulder and a NASA Exobiology Grant (80NSSC17K0667) to S.H.K. The authors would like to thank Daniel Sigman for support and access to analytical instrumentation at Princeton University. The authors are grateful to Emma Kast, Dario Marconi, Sergey Oleynik, and other members of the Sigman Lab for providing guidance and

support throughout sample processing and isotopic analysis. The authors thank three anonymous reviewers for their insightful comments that improved the quality of this manuscript. We also sincerely thank the Dietrich Lab for providing us with the *P. aeruginosa* mutant strains.

## ■ REFERENCES

- (1) Gruber, N.; Galloway, J. N. An Earth-System Perspective of the Global Nitrogen Cycle. *Nature* **2008**, *451*, 293–296.
- (2) Haber, F. The Synthesis of Ammonia from Its Elements, Nobel Lecture. *Resonance* **2002**, *7*, 86–94.
- (3) Simon, J.; Klotz, M. G. Diversity and Evolution of Bioenergetic Systems Involved in Microbial Nitrogen Compound Transformations. *Biochim. Biophys. Acta* **2013**, *1827*, 114–135.
- (4) Brunner, B.; Contreras, S.; Lehmann, M. F.; Matantseva, O.; Rollog, M.; Kalvelage, T.; Klockgether, G.; Lavik, G.; Jetten, M. S. M.; Kartal, B.; Kuypers, M. M. M. Nitrogen Isotope Effects Induced by Anammox Bacteria. *Proc. Natl. Acad. Sci. U.S.A.* **2013**, *110*, 18994–18999.
- (5) Buchwald, C.; Casciotti, K. L. Oxygen Isotopic Fractionation and Exchange during Bacterial Nitrite Oxidation. *Limnol. Oceanogr.* **2010**, *55*, 1064–1074.
- (6) Casciotti, K. L. Inverse Kinetic Isotope Fractionation during Bacterial Nitrite Oxidation. *Geochim. Cosmochim. Acta* **2009**, *73*, 2061–2076.
- (7) Granger, J.; Sigman, D. M.; Lehmann, M. F.; Tortell, P. D. Nitrogen and Oxygen Isotope Fractionation during Dissimilatory Nitrate Reduction by Denitrifying Bacteria. *Limnol. Oceanogr.* **2008**, *53*, 2533–2545.
- (8) Kobayashi, K.; Makabe, A.; Yano, M.; Oshiki, M.; Kindaichi, T.; Casciotti, K. L.; Okabe, S. Dual Nitrogen and Oxygen Isotope Fractionation during Anaerobic Ammonium Oxidation by Anammox Bacteria. *ISME J.* **2019**, *13*, 2426–2436.
- (9) Zhang, X.; Sigman, D. M.; Morel, F. M. M.; Kraepiel, A. M. L. Nitrogen Isotope Fractionation by Alternative Nitrogenases and Past Ocean Anoxia. *Proc. Natl. Acad. Sci. U.S.A.* **2014**, *111*, 4782–4787.
- (10) Bauersachs, T.; Schouten, S.; Compaoré, J.; Wollenzien, U.; Stal, L. J.; Damsteé, J. S. S. Nitrogen Isotopic Fractionation Associated with Growth on Dinitrogen Gas and Nitrate by Cyanobacteria. *Limnol. Oceanogr.* **2009**, *54*, 1403–1411.
- (11) Carpenter, E. J.; Harvey, H. R.; Fry, B.; Capone, D. G. Biogeochemical Tracers of the Marine *Cyanobacterium trichodesmium*. *Deep Sea Res., Part I* **1997**, *44*, 27–38.
- (12) Macko, S. A.; Fogel, M. L.; Hare, P. E.; Hoering, T. C. Isotopic Fractionation of Nitrogen and Carbon in the Synthesis of Amino Acids by Microorganisms. *Chem. Geol.* **1987**, *65*, 79–92.
- (13) Minagawa, M.; Wada, E. Nitrogen Isotope Ratios of Red Tide Organisms in the East China Sea: A Characterization of Biological Nitrogen Fixation. *Mar. Chem.* **1986**, *19*, 245–259.
- (14) González, P. J.; Correia, C.; Moura, I.; Brondino, C. D.; Moura, J. J. G. Bacterial Nitrate Reductases: Molecular and Biological Aspects of Nitrate Reduction. *J. Inorg. Biochem.* **2006**, *100*, 1015–1023.
- (15) Kraft, B.; Strous, M.; Tegetmeyer, H. E. Microbial Nitrate Respiration – Genes, Enzymes and Environmental Distribution. *J. Biotechnol.* **2011**, *155*, 104–117.
- (16) Goddard, A. D.; Bali, S.; Mavridou, D. A. I.; Luque-Almagro, V. M.; Gates, A. J.; Roldán, M. D.; Newstead, S.; Richardson, D. J.; Ferguson, S. J. The *Paracoccus denitrificans* NarK-like Nitrate and Nitrite Transporters-Probing Nitrate Uptake and Nitrate/Nitrite Exchange Mechanisms: Nitrate and Nitrite Transport in *Paracoccus denitrificans*. *Mol. Microbiol.* **2017**, *103*, 117–133.
- (17) Bourbonnais, A.; Letscher, R. T.; Bange, H. W.; Échevin, V.; Larkum, J.; Mohn, J.; Yoshida, N.; Altabet, M. A. N<sub>2</sub> O Production and Consumption from Stable Isotopic and Concentration Data in the Peruvian Coastal Upwelling System: N<sub>2</sub>O Production and Consumption off Peru. *Global Biogeochem. Cycles* **2017**, *31*, 678–698.
- (18) Casciotti, K. L.; Buchwald, C.; McIlvin, M. Implications of Nitrate and Nitrite Isotopic Measurements for the Mechanisms of Nitrogen Cycling in the Peru Oxygen Deficient Zone. *Deep Sea Res., Part I* **2013**, *80*, 78–93.
- (19) Casciotti, K. L.; McIlvin, M. R. Isotopic Analyses of Nitrate and Nitrite from Reference Mixtures and Application to Eastern Tropical North Pacific Waters. *Mar. Chem.* **2007**, *107*, 184–201.
- (20) DiFiore, P. J.; Sigman, D. M.; Dunbar, R. B. Upper Ocean Nitrogen Fluxes in the Polar Antarctic Zone: Constraints from the Nitrogen and Oxygen Isotopes of Nitrate: Polar Antarctic Nitrate N and O Isotopes. *Geochim. Geophys. Geosyst.* **2009**, *10*, 1–22.
- (21) Gaye, B.; Nagel, B.; Dähnke, K.; Rixen, T.; Emeis, K.-C. Evidence of Parallel Denitrification and Nitrite Oxidation in the ODZ of the Arabian Sea from Paired Stable Isotopes of Nitrate and Nitrite. *Global Biogeochem. Cycles* **2013**, *27*, 1059–1071.
- (22) Rafter, P. A.; DiFiore, P. J.; Sigman, D. M. Coupled Nitrate Nitrogen and Oxygen Isotopes and Organic Matter Remineralization in the Southern and Pacific Oceans: Nitrate Isotopes and Remineralization. *J. Geophys. Res.* **2013**, *118*, 4781–4794.
- (23) Aravena, R.; Robertson, W. D. Use of Multiple Isotope Tracers to Evaluate Denitrification in Ground Water: Study of Nitrate from a Large-Flux Septic System Plume. *Ground Water* **1998**, *36*, 975–982.
- (24) Böttcher, J.; Strebel, O.; Voerkelius, S.; Schmidt, H.-L. Using Isotope Fractionation of Nitrate-Nitrogen and Nitrate-Oxygen for Evaluation of Microbial Denitrification in a Sandy Aquifer. *J. Hydrol.* **1990**, *114*, 413–424.
- (25) Houlton, B. Z.; Sigman, D. M.; Hedin, L. O. Isotopic Evidence for Large Gaseous Nitrogen Losses from Tropical Rainforests. *Proc. Natl. Acad. Sci. U.S.A.* **2006**, *103*, 8745–8750.
- (26) Mengis, M.; Schiff, S. L.; Harris, M.; English, M. C.; Aravena, R.; Elgood, R. J.; MacLean, A. Multiple Geochemical and Isotopic Approaches for Assessing Ground Water NO<sub>3</sub><sup>−</sup> Elimination in a Riparian Zone. *Ground Water* **1999**, *37*, 448–457.
- (27) Wenk, C. B.; Zopfi, J.; Bles, J.; Veronesi, M.; Niemann, H.; Lehmann, M. F. Community N and O Isotope Fractionation by Sulfide-Dependent Denitrification and Anammox in a Stratified Lacustrine Water Column. *Geochim. Cosmochim. Acta* **2014**, *125*, 551–563.
- (28) Lehmann, M. F.; Reichert, P.; Bernasconi, S. M.; Barbieri, A.; McKenzie, J. A. Modelling Nitrogen and Oxygen Isotope Fractionation during Denitrification in a Lacustrine Redox-Transition Zone. *Geochim. Cosmochim. Acta* **2003**, *67*, 2529–2542.
- (29) Cey, E. E.; Rudolph, D. L.; Aravena, R.; Parkin, G. Role of the Riparian Zone in Controlling the Distribution and Fate of Agricultural Nitrogen near a Small Stream in Southern Ontario. *J. Contam. Hydrol.* **1999**, *37*, 45–67.
- (30) Granger, J.; Wankel, S. D. Isotopic Overprinting of Nitrification on Denitrification as a Ubiquitous and Unifying Feature of Environmental Nitrogen Cycling. *Proc. Natl. Acad. Sci. U.S.A.* **2016**, *113*, E6391–E6400.
- (31) Philippot, L. Denitrifying Genes in Bacterial and Archaeal Genomes. *Biochim. Biophys. Acta* **2002**, *1577*, 355–376.
- (32) Richardson, D. J.; Berks, B. C.; Russell, D. A.; Spiro, S.; Taylor, C. J. Functional, Biochemical and Genetic Diversity of Prokaryotic Nitrate Reductases. *Cell. Mol. Life Sci.* **2001**, *58*, 165–178.
- (33) Frey, C.; Hietanen, S.; Jürgens, K.; Labrenz, M.; Voss, M. N and O Isotope Fractionation in Nitrate during Chemolithoautotrophic Denitrification by *Sulfurimonas gotlandica*. *Environ. Sci. Technol.* **2014**, *48*, 13229–13237.
- (34) Treibergs, L. A.; Granger, J. Enzyme Level N and O Isotope Effects of Assimilatory and Dissimilatory Nitrate Reduction. *Limnol. Oceanogr.* **2017**, *62*, 272–288.
- (35) Kritee, K.; Sigman, D. M.; Granger, J.; Ward, B. B.; Jayakumar, A.; Deutsch, C. Reduced Isotope Fractionation by Denitrification under Conditions Relevant to the Ocean. *Geochim. Cosmochim. Acta* **2012**, *92*, 243–259.
- (36) Wunderlich, A.; Meckenstock, R.; Einsiedl, F. Effect of Different Carbon Substrates on Nitrate Stable Isotope Fractionation During Microbial Denitrification. *Environ. Sci. Technol.* **2012**, *46*, 4861–4868.

- (37) Rahme, L.; Stevens, E.; Wolfort, S.; Shao, J.; Tompkins, R.; Ausubel, F. Common Virulence Factors for Bacterial Pathogenicity in Plants and Animals. *Science* **1995**, *268*, 1899–1902.
- (38) Rainey, F. A.; Stakebrandt, E.; Brghardt, J.; et al. A Re-Evaluation of the Taxonomy of *Paracoccus denitrificans* and a Proposal for the Combination *Paracoccus pantotrophus* Comb. Nov. *Int. J. Syst. Evol. Microbiol.* **1999**, *49*, 645–651.
- (39) Beijerinck, M. W. Über Spirillum Desulfuricans Als Ursache von Sulfatreduktion. *Zentralbl. Bakteriol.* **1895**, *1*, 1–9.
- (40) Gao, H.; et al. *Shewanella loihica* Sp. Nov., Isolated from Iron-Rich Microbial Mats in the Pacific Ocean. *Int. J. Syst. Evol. Microbiol.* **2006**, *56*, 1911–1916.
- (41) Kluyver, A. J.; Van Niel, C. B. Prospects for a Natural System of Classification of Bacteria. *Zentralbl. Bakteriol., Parasitenkd., Infektion-skrankh. Hyg.* **1936**, *94*, 369–403.
- (42) Dietrich, L. E. P.; Okegbe, C.; Price-Whelan, A.; Sakhtah, H.; Hunter, R. C.; Newman, D. K. Bacterial Community Morphogenesis Is Intimately Linked to the Intracellular Redox State. *J. Bacteriol.* **2013**, *195*, 1371–1380.
- (43) Heyrman, J.; Vanparys, B.; Logan, N. A.; Balcaen, A.; Rodríguez-Díaz, M.; Felske, A.; De Vos, P. *Bacillus novalis* Sp. Nov., *Bacillus viresi* Sp. Nov., *Bacillus soli* Sp. Nov., *Bacillus bataviensis* Sp. Nov. and *Bacillus drenensis* Sp. Nov., from the Drentse A Grasslands. *Int. J. Syst. Evol. Microbiol.* **2004**, *54*, 47–57.
- (44) Neidhardt, F. C.; Bloch, P. L.; Smith, D. F. Culture Medium for Enterobacteria. *J. Bacteriol.* **1974**, *119*, 736–747.
- (45) Mania, D.; Heylen, K.; van Spanning, R. J. M.; Frostegård, Å. The Nitrate-Ammonifying and *NosZ* -Carrying Bacterium *Bacillus viresi* Is a Potent Source and Sink for Nitric and Nitrous Oxide under High Nitrate Conditions: *Bacillus viresi* Is a Source and Sink for NO and N<sub>2</sub>O. *Environ. Microbiol.* **2014**, *16*, 3196–3210.
- (46) Postgate, J. R. Versatile Medium for the Enumeration of Sulfate-Reducing Bacteria. *Appl. Microbiol.* **1963**, *11*, 265–267.
- (47) Yoon, S.; Cruz-García, C.; Sanford, R.; Ritalahti, K. M.; Löffler, F. E. Denitrification versus Respiratory Ammonification: Environmental Controls of Two Competing Dissimilatory NO<sub>3</sub><sup>-</sup>/NO<sub>2</sub><sup>-</sup> Reduction Pathways in *Shewanella loihica* Strain PV-4. *ISME J.* **2015**, *9*, 1093–1104.
- (48) Hahnke, S. M.; Moosmann, P.; Erb, T. J.; Strous, M. An Improved Medium for the Anaerobic Growth of *Paracoccus denitrificans* Pd1222. *Front. Microbiol.* **2014**, *5*, No. 18.
- (49) Sigman, D. M.; Casciotti, K. L.; Andreani, M.; Barford, C.; Galanter, M.; Böhlke, J. K. A Bacterial Method for the Nitrogen Isotopic Analysis of Nitrate in Seawater and Freshwater. *Anal. Chem.* **2001**, *73*, 4145–4153.
- (50) Weigand, M. A.; Foriel, J.; Barnett, B.; Oleynik, S.; Sigman, D. M. Updates to Instrumentation and Protocols for Isotopic Analysis of Nitrate by the Denitrifier Method: Denitrifier Method Protocols and Instrumentation Updates. *Rapid Commun. Mass Spectrom.* **2016**, *30*, 1365–1383.
- (51) Granger, J.; Sigman, D. M. Removal of Nitrite with Sulfamic Acid for Nitrate N and O Isotope Analysis with the Denitrifier Method. *Rapid Commun. Mass Spectrom.* **2009**, *23*, 3753–3762.
- (52) Coplen, T. B. Guidelines and Recommended Terms for Expression of Stable-Isotope-Ratio and Gas-Ratio Measurement Results: Guidelines and Recommended Terms for Expressing Stable Isotope Results. *Rapid Commun. Mass Spectrom.* **2011**, *25*, 2538–2560.
- (53) Mariotti, A.; Germon, J. C.; Hubert, P.; Kaiser, P.; Letolle, R.; Tardieu, A.; Tardieu, P. Experimental Determination of Nitrogen Kinetic Isotope Fractionation: Some Principles; Illustration for the Denitrification and Nitrification Processes. *Plant Soil* **1981**, *62*, 413–430.
- (54) Sievers, F.; Wilm, A.; Dineen, D.; Gibson, T. J.; Karplus, K.; Li, W.; Lopez, R.; McWilliam, H.; Remmert, M.; Söding, J.; Thompson, J. D.; Higgins, D. G. Fast, Scalable Generation of High-Quality Protein Multiple Sequence Alignments Using Clustal Omega. *Mol. Syst. Biol.* **2011**, *7*, 539.
- (55) Huelsenbeck, J. P.; Ronquist, F. MRBAYES: Bayesian Inference of Phylogenetic Trees. *Bioinformatics* **2001**, *17*, 754–755.
- (56) Carlisle, E.; Yarnes, C.; Toney, M. D.; Bloom, A. J. Nitrate Reductase 15N Discrimination in *Arabidopsis thaliana*, *Zea mays*, *Aspergillus niger*, *Picea angusta*, and *Escherichia coli*. *Front. Plant Sci.* **2014**, *5*, No. 317.
- (57) Ellington, M. J. K.; Bhakoo, K. K.; Sawers, G.; Richardson, D. J.; Ferguson, S. J. Hierarchy of Carbon Source Selection in *Paracoccus pantotrophus*: Strict Correlation between Reduction State of the Carbon Substrate and Aerobic Expression of the Nap Operon. *J. Bacteriol.* **2002**, *184*, 4767–4774.
- (58) Sears, H. J.; Sawers, G.; Berks, B. C.; Ferguson, S. J.; Richardson, D. J. Control of Periplasmic Nitrate Reductase Gene Expression (NapEDABC) from *Paracoccus Pantotrophus* in Response to Oxygen and Carbon Substrates. *Microbiology* **2000**, *146*, 2977–2985.
- (59) Sears, H. J.; Spiro, S.; Richardson, D. J. Effect of Carbon Substrate and Aeration on Nitrate Reduction and Expression of the Periplasmic and Membrane-Bound Nitrate Reductases in Carbon-Limited Continuous Cultures of *Paracoccus denitrificans* Pd1222. *Microbiology* **1997**, *143*, 3767–3774.
- (60) Sears, H. J.; Ferguson, S. J.; Richardson, D. J.; Spiro, S. The Identification of a Periplasmic Nitrate Reductase in *Paracoccus denitrificans*. *FEMS Microbiol. Lett.* **1993**, *113*, 107–111.
- (61) Barford, C. C.; Montoya, J. P.; Altabet, M. A.; Mitchell, R. Steady-State Nitrogen Isotope Effects of N<sub>2</sub> and N<sub>2</sub>O Production in *Paracoccus denitrificans*. *Appl. Environ. Microbiol.* **1999**, *65*, 989–994.
- (62) Cabello, P.; Roldán, M. D.; Moreno-Vivián, C. Nitrate Reduction and the Nitrogen Cycle in Archaea. *Microbiology* **2004**, *150*, 3527–3546.
- (63) Heylen, K.; Keltjens, J. Redundancy and Modularity in Membrane-Associated Dissimilatory Nitrate Reduction in *Bacillus*. *Front. Microbiol.* **2012**, *3*, No. 71.
- (64) Bedzyk, L.; Wang, T.; Ye, R. W. The Periplasmic Nitrate Reductase In *Pseudomonas* Sp. Strain G-179 Catalyzes the First Step of Denitrification. *J. Bacteriol.* **1999**, *181*, 2802–2806.
- (65) Ji, B.; Yang, K.; Zhu, L.; Jiang, Y.; Wang, H.; Zhou, J.; Zhang, H. Aerobic Denitrification: A Review of Important Advances of the Last 30 Years. *Biotechnol. Bioprocess Eng.* **2015**, *20*, 643–651.
- (66) Li, Y.; Katzmann, E.; Borg, S.; Schüler, D. The Periplasmic Nitrate Reductase Nap Is Required for Anaerobic Growth and Involved in Redox Control of Magnetite Biomineralization in *Magnetospirillum gryphiswaldense*. *J. Bacteriol.* **2012**, *194*, 4847–4856.
- (67) Potter, L. C.; Millington, P.; Griffiths, L.; Thomas, G. H.; Cole, J. A. Competition between *Escherichia coli* Strains Expressing Either a Periplasmic or a Membrane-Bound Nitrate Reductase: Does Nap Confer a Selective Advantage during Nitrate-Limited Growth? *Biochem. J.* **1999**, *344*, 77–84.
- (68) Stewart, V.; Lu, Y.; Darwin, A. J. Periplasmic Nitrate Reductase (NapABC Enzyme) Supports Anaerobic Respiration by *Escherichia coli* K-12. *J. Bacteriol.* **2002**, *184*, 1314–1323.
- (69) Sparacino-Watkins, C.; Stolz, J. F.; Basu, P. Nitrate and Periplasmic Nitrate Reductases. *Chem. Soc. Rev.* **2014**, *43*, 676–706.
- (70) Dong, Y.; Wang, J.; Fu, H.; Zhou, G.; Shi, M.; Gao, H. A Crp-Dependent Two-Component System Regulates Nitrate and Nitrite Respiration in *Shewanella oneidensis*. *PLoS One* **2012**, *7*, No. e51643.
- (71) Mesa, S.; Hauser, F.; Friberg, M.; Malaguti, E.; Fischer, H.-M.; Hennecke, H. Comprehensive Assessment of the Regulons Controlled by the FixLJ-FixK2-FixK1 Cascade in *Bradyrhizobium japonicum*. *J. Bacteriol.* **2008**, *190*, 6568–6579.
- (72) Robles, E. F.; Sánchez, C.; Bonnard, N.; Delgado, M. J.; Bedmar, E. J. The *Bradyrhizobium japonicum* NapEDABC Genes Are Controlled by the FixLJ-FixK2-NnrR Regulatory Cascade. *Biochem. Soc. Trans.* **2006**, *34*, 108–110.
- (73) Stewart, V. Regulation of Nitrate and Nitrite Reductase Synthesis in Enterobacteria. *Antonie Van Leeuwenhoek* **1994**, *66*, 37–45.
- (74) Lin, Y.-C.; Sekedat, M. D.; Cornell, W. C.; Silva, G. M.; Okegbe, C.; Price-Whelan, A.; Vogel, C.; Dietrich, L. E. P. Phenazines

Regulate Nap-Dependent Denitrification in *Pseudomonas aeruginosa* Biofilms. *J. Bacteriol.* **2018**, 200, No. e00031-18.

(75) Sezonov, G.; Joseleau-Petit, D.; D'Ari, R. *Escherichia coli* Physiology in Luria–Bertani Broth. *J. Bacteriol.* **2007**, 189, 8746–8749.

(76) Morozkina, E. V.; Zvyagil'skaya, R. A. Nitrate Reductases: Structure, Functions, and Effect of Stress Factors. *Biochemistry* **2007**, 72, 1151–1160.

(77) Barford, D. The Role of Cysteine Residues as Redox-Sensitive Regulatory Switches. *Curr. Opin. Struct. Biol.* **2004**, 14, 679–686.

(78) Coelho, C.; Romão, M. J. Structural and Mechanistic Insights on Nitrate Reductases. *Protein Sci.* **2015**, 24, 1901–1911.

(79) Wirtz, M.; Droux, M. Synthesis of the Sulfur Amino Acids: Cysteine and Methionine. *Photosynth. Res.* **2005**, 86, 345–362.

(80) Arnoux, P.; Sabaty, M.; Alric, J.; Frangioni, B.; Guigliarelli, B.; Adriano, J.-M.; Pignol, D. Structural and Redox Plasticity in the Heterodimeric Periplasmic Nitrate Reductase. *Nat. Struct. Mol. Biol.* **2003**, 10, 928–934.

(81) Gates, A. J.; Richardson, D. J.; Butt, J. N. Voltammetric Characterization of the Aerobic Energy-Dissipating Nitrate Reductase of *Paracoccus pantotrophus*: Exploring the Activity of a Redox-Balancing Enzyme as a Function of Electrochemical Potential. *Biochem. J.* **2008**, 409, 159–168.

(82) Pinho, D.; Besson, S.; Silva, P. J.; de Castro, B.; Moura, I. Isolation and Spectroscopic Characterization of the Membrane-Bound Nitrate Reductase from *Pseudomonas chlororaphis* DSM 50135. *Biochim. Biophys. Acta* **2005**, 1723, 151–162.

(83) Najmudin, S.; González, P. J.; Trincão, J.; Coelho, C.; Mukhopadhyay, A.; Cerqueira, N. M. F. S. A.; Romão, C. C.; Moura, I.; Moura, J. J. G.; Brondino, C. D.; Romão, M. J. Periplasmic Nitrate Reductase Revisited: A Sulfur Atom Completes the Sixth Coordination of the Catalytic Molybdenum. *J. Biol. Inorg. Chem.* **2008**, 13, 737–753.

(84) Jormakka, M.; Richardson, D.; Byrne, B.; Iwata, S. Architecture of NarGH Reveals a Structural Classification of Mo-BisMGD Enzymes. *Structure* **2004**, 12, 95–104.

(85) Anderson, L. J.; Richardson, D. J.; Butt, J. N. Catalytic Protein Film Voltammetry from a Respiratory Nitrate Reductase Provides Evidence for Complex Electrochemical Modulation of Enzyme Activity. *Biochemistry* **2001**, 40, 11294–11307.

(86) Marangon, J.; de Sousa, P. M. P.; Moura, I.; Brondino, C. D.; Moura, J. J. G.; González, P. J. Substrate-Dependent Modulation of the Enzymatic Catalytic Activity: Reduction of Nitrate, Chlorate and Perchlorate by Respiratory Nitrate Reductase from *Marinobacter hydrocarbonoclasticus* 617. *Biochim. Biophys. Acta* **2012**, 1817, 1072–1082.

(87) Husson, O. Redox Potential (Eh) and PH as Drivers of Soil/Plant/Microorganism Systems: A Transdisciplinary Overview Pointing to Integrative Opportunities for Agronomy. *Plant Soil* **2013**, 362, 389–417.

(88) Spiro, S.; Guest, J. R. FNR and Its Role in Oxygen-Regulated Gene Expression in *Escherichia coli*. *FEMS Microbiol. Rev.* **1990**, 6, 399–428.

(89) Moir, J. W. B.; Wood, N. J. Nitrate and Nitrite Transport in Bacteria. *Cell. Mol. Life Sci.* **2001**, 58, 215–224.

(90) Wood, N. J.; Alizadeh, T.; Bennett, S.; Pearce, J.; Ferguson, S. J.; Richardson, D. J.; Moir, J. W. B. Maximal Expression of Membrane-Bound Nitrate Reductase in *Paracoccus* Is Induced by Nitrate via a Third FNR-Like Regulator Named NarR. *J. Bacteriol.* **2001**, 183, 3606–3613.

(91) Lam, P.; Kuypers, M. M. M. Microbial Nitrogen Cycling Processes in Oxygen Minimum Zones. *Annu. Rev. Mar. Sci.* **2011**, 3, 317–345.

(92) Ulloa, O.; Canfield, D. E.; DeLong, E. F.; Letelier, R. M.; Stewart, F. J. Microbial Oceanography of Anoxic Oxygen Minimum Zones. *Proc. Natl. Acad. Sci. U.S.A.* **2012**, 109, 15996–16003.

(93) Bru, D.; Sarr, A.; Philippot, L. Relative Abundances of Proteobacterial Membrane-Bound and Periplasmic Nitrate Reduc-

tases in Selected Environments. *Appl. Environ. Microbiol.* **2007**, 73, 5971–5974.

(94) Smith, C. J.; Nedwell, D. B.; Dong, L. F.; Osborn, A. M. Diversity and Abundance of Nitrate Reductase Genes (NarG and NapA), Nitrite Reductase Genes (NirS and NirX), and Their Transcripts in Estuarine Sediments. *Appl. Environ. Microbiol.* **2007**, 73, 3612–3622.

(95) Dong, L. F.; Smith, C. J.; Papaspyrou, S.; Stott, A.; Osborn, A. M.; Nedwell, D. B. Changes in Benthic Denitrification, Nitrate Ammonification, and Anammox Process Rates and Nitrate and Nitrite Reductase Gene Abundances along an Estuarine Nutrient Gradient (the Colne Estuary, United Kingdom). *Appl. Environ. Microbiol.* **2009**, 75, 3171–3179.

(96) Verbaendert, I.; Boon, N.; De Vos, P.; Heylen, K. Denitrification Is a Common Feature among Members of the Genus *Bacillus*. *Syst. Appl. Microbiol.* **2011**, 34, 385–391.

(97) Chen, Y.; Wang, F.; Xu, J.; Mehmood, M. A.; Xiao, X. Physiological and Evolutionary Studies of NAP Systems in *Shewanella piezotolerans* WP3. *ISME J.* **2011**, 5, 843–855.

(98) Kiss, H.; Lang, E.; Lapidus, A.; Copeland, A.; Nolan, M.; Glavina Del Rio, T.; Chen, F.; Lucas, S.; Tice, H.; Cheng, J.-F.; Han, C.; Goodwin, L.; Pitluck, S.; Liolios, K.; Pati, A.; Ivanova, N.; Mavromatis, K.; Chen, A.; Palaniappan, K.; Land, M.; Hauser, L.; Chang, Y.-J.; Jeffries, C. D.; Detter, J. C.; Brettin, T.; Spring, S.; Rohde, M.; Göker, M.; Woyke, T.; Bristow, J.; Eisen, J. A.; Markowitz, V.; Hugenholtz, P.; Kyrpides, N. C.; Klenk, H.-P. Complete Genome Sequence of *Denitrovibrio acetiphilus* Type Strain (N2460T). *Stand. Genomic Sci.* **2010**, 2, 270–279.

(99) Rusmana, I.; Nedwell, D. B. Use of Chlorate as a Selective Inhibitor to Distinguish Membrane-Bound Nitrate Reductase (Nar) and Periplasmic Nitrate Reductase (Nap) of Dissimilative Nitrate Reducing Bacteria in Sediment. *FEMS Microbiol. Ecol.* **2004**, 48, 379–386.

## **Supporting information for:** Enzyme specific coupling of oxygen and nitrogen isotope fractionation of the Nap and Nar nitrate reductases

Ciara K. Asamoto<sup>1\*</sup>, Kaitlin R. Rempfert<sup>1</sup>, Victoria H. Luu<sup>2</sup>, Adam D. Younkin<sup>1</sup>, Sebastian H. Kopf<sup>1</sup>

<sup>1</sup>Department of Geological Sciences, University of Colorado Boulder, Boulder, CO 80309

<sup>2</sup>Department of Geosciences, Princeton University, Princeton, NJ 08544

**Content:** Pages S1-S18. SI Table 1, Figures S1-S6, and supplemental discussion on impacts of nitrite accumulation and information about data collection for Fig. 1.

**Table S1. Data Summary.**

Summary of  $^{18}\epsilon$  /  $^{15}\epsilon$  coupling, fractionation factor, and growth rate estimates by organism and medium. Each row represents a single culture. Fractionation factors calculated from Rayleigh distillation regressions (see Fig. S3 and Fig. S4). Biological replicates with fewer than three isotopic data points were not included.  $^{18}\epsilon$  /  $^{15}\epsilon$  coupling values were calculated using regressions across all cultures from the same medium (see Fig. S5).

Species	Reductase genes	Medium	$^{18}\epsilon$ / $^{15}\epsilon$	$^{15}\epsilon$ +/- std. err (%)	$^{18}\epsilon$ +/- std. err (%)	Growth Rate (hr <sup>-1</sup> ) +/- std. err
<i>B. bataviensis</i>	narG	TSB	0.61 +/- 0.06	-15.4 +/- 1.6 -13.6 +/- 2.0 -11.8 +/- 2.1	-10.4 +/- 0.7 -5.2 +/- 2.1 -8.1 +/- 0.7	0.31 +/- 0.10 0.24 +/- 0.07 0.24 +/- 0.06
<i>B. vireti</i>	narG	TSB TSB + $^{18}\text{O}$ water	0.64 +/- 0.04	-10.8 +/- 3.5 -12.6 +/- 5.7 -21.3 +/- 3.2 -21.0 +/- 3.6 -10.9 +/- 4.6	-9.7 +/- 2.1 -9.3 +/- 4.1 -11.4 +/- 2.8 -13.1 +/- 2.2 -6.3 +/- 2.6	0.55 +/- 0.05 0.56 +/- 0.04
<i>D. desulfuricans</i>	napA	Postgate	0.63 +/- 0.06	-22.0 +/- 0.4 -24.1 +/- 1.2 -24.8 +/- 1.4	-13.9 +/- 3.1 -15.2 +/- 2.4 -15.8 +/- 3.3	
<i>P. aeruginosa</i> WT	both	LB LB + $^{18}\text{O}$ water MOPS	0.97 +/- 0.02 0.63 +/- 0.02	-28.4 +/- 1.2 -27.7 +/- 0.5 -28.5 +/- 0.6 -22.6 +/- 2.4 -26.8 +/- 0.4 -23.5 +/- 2.2 -23.4 +/- 0.9 -22.5 +/- 1.0 -23.0 +/- 0.4	-26.2 +/- 1.4 -25.8 +/- 0.9 -26.8 +/- 0.8 -21.8 +/- 2.2 -24.5 +/- 1.3 -24.5 +/- 1.4 -15.3 +/- 1.2 -14.3 +/- 1.8 -14.1 +/- 1.2	0.11 +/- 0.04 0.10 +/- 0.04 0.11 +/- 0.03 0.05 +/- 0.02 0.06 +/- 0.02 0.09 +/- 0.01 0.12 +/- 0.03 0.14 +/- 0.03 0.11 +/- 0.00
<i>P. aeruginosa</i> $\Delta$ napA	narG	LB LB + $^{18}\text{O}$ water MOPS	0.91 +/- 0.01 0.85 +/- 0.02	-24.9 +/- 2.0 -28.8 +/- 2.9 -26.7 +/- 0.3 -26.5 +/- 0.7 -27.5 +/- 0.4 -26.1 +/- 0.3 -24.7 +/- 0.5 -23.8 +/- 1.9	-22.7 +/- 1.8 -26.2 +/- 2.7 -24.3 +/- 1.0 -24.0 +/- 1.4 -23.6 +/- 1.0 -22.4 +/- 1.2 -20.4 +/- 1.6 -20.4 +/- 0.7	0.09 +/- 0.01 0.09 +/- 0.01 0.09 +/- 0.01 0.09 +/- 0.01 0.10 +/- 0.01 0.09 +/- 0.02 0.07 +/- 0.01 0.08 +/- 0.01
<i>P. aeruginosa</i> $\Delta$ narG	napA	LB LB + $^{18}\text{O}$ water	0.49 +/- 0.00	-31.8 +/- 0.4 -32.2 +/- 0.1 -33.8 +/- 2.4 -34.7 +/- 0.8 -33.2 +/- 0.5 -34.8 +/- 0.5	-15.4 +/- 0.4 -15.3 +/- 0.0 -16.1 +/- 1.6 -17.4 +/- 0.2 -15.7 +/- 0.5 -17.5 +/- 0.2	0.46 +/- 0.20 0.41 +/- 0.11 0.39 +/- 0.16 0.11 +/- 0.04
<i>P. denitrificans</i>	both	Hahnke	0.92 +/- 0.01	-16.9 +/- 1.4 -16.7 +/- 0.9 -17.0 +/- 0.6	-15.7 +/- 1.2 -15.4 +/- 0.7 -15.3 +/- 0.6	0.24 +/- 0.04 0.27 +/- 0.01 0.24 +/- 0.02
<i>S. loihica</i>	napA	SL	0.55 +/- 0.01	-21.8 +/- 0.3 -20.8 +/- 2.6	-12.2 +/- 0.4 -11.7 +/- 0.2	

**Table S2. Gene accession numbers.**

A list of NCBI gene accession numbers used in phylogenetic analyses. In some bacteria two copies of napA exist and thus the analysis was run twice to determine any changes to tree topology. No significant change to the resulting phylogenetic tree occurred. The (\*) denotes which gene was used in the final analysis.

Name	Gene	Gene accession number
<i>Aromatoleum aromaticum</i> EbN1	Nar	WP_011239378.1
<i>Paracoccus denitrificans</i> PD1222	Nar	WP_011750465.1
<i>Bacillus bataviensis</i> LMG 21833	Nar	EKN65800.1
<i>Pseudomonas aeruginosa</i> PA14	Nar	EOT11604.1
<i>Bacillus vireti</i> LMG 21834	Nar	ETI68959.1
<i>Pseudomonas chlororaphis chlororaphis</i> ATCC 9446	Nar	WP_124303001.1
<i>Thauera aromatica</i> K172	Nar	WP_107220859.1
<i>Paracoccus denitrificans</i> PD1222	Nap	WP_011750941.1
<i>Rhodobacter sphaeroides</i> ATCC 17025	Nap	WP_011910165.1
<i>Rhodobacter sphaeroides</i> ATCC 17025	Nap	WP_011911096.1*
<i>Shewanella loihica</i> PV-4	Nap	WP_011867002.1*
<i>Shewanella loihica</i> PV-4	Nap	WP_041407111.1
<i>Sulfurimonas gotlandica</i> GD1	Nap	WP_008337904.1
<i>Desulfovibrio desulfuricans desulfuricans</i> DSM 642	Nap	WP_022659785.1

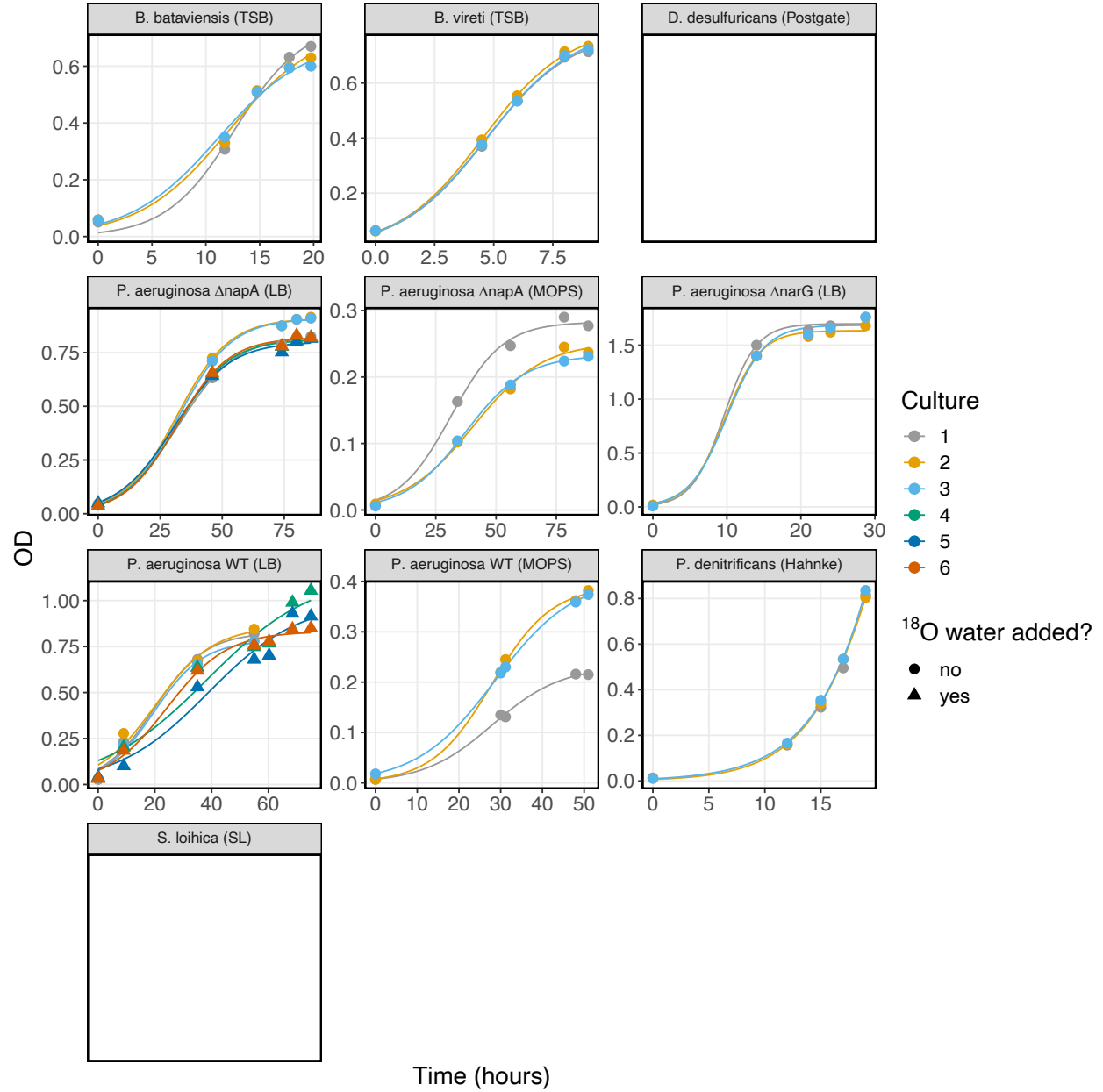
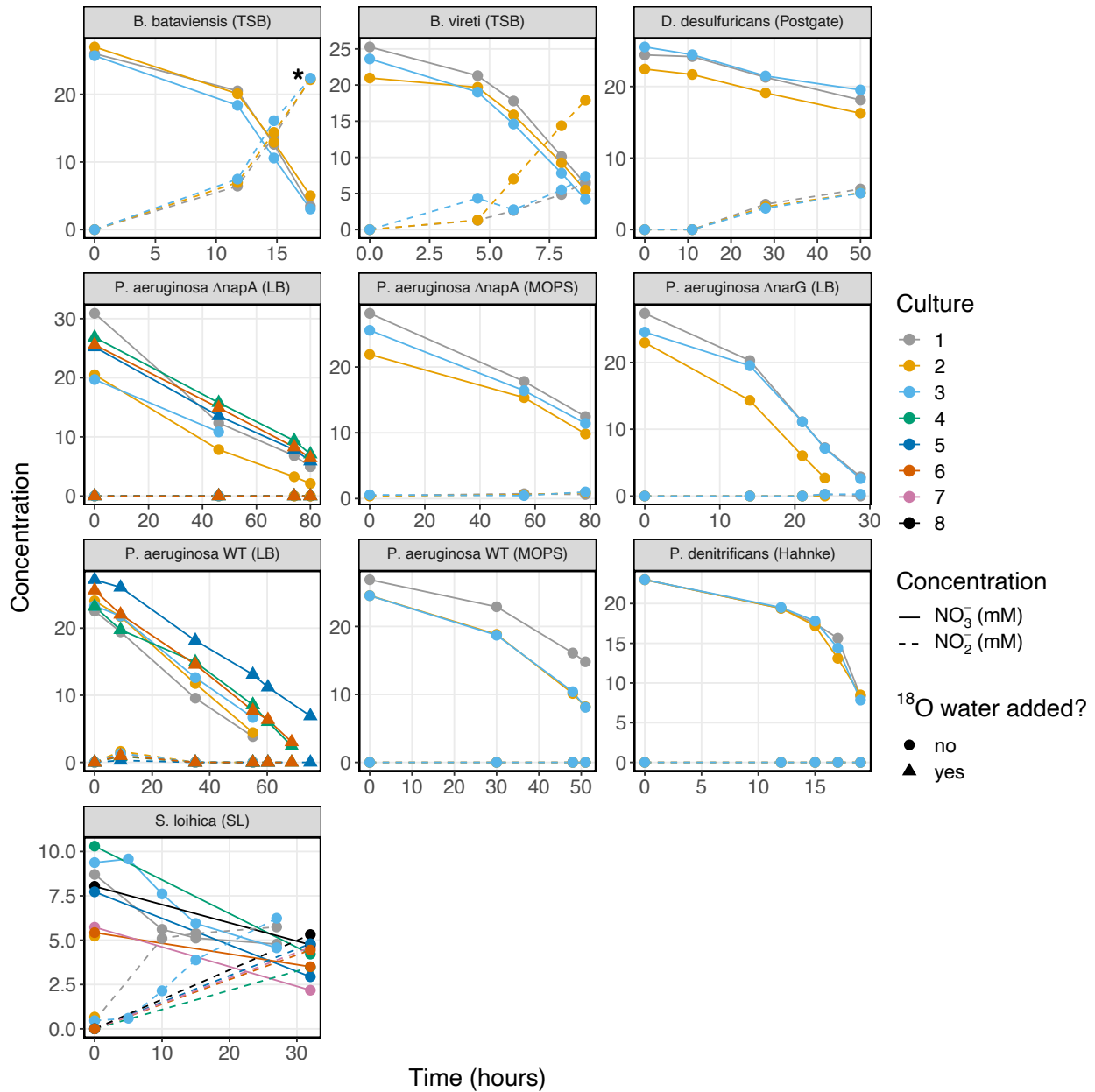


**Figure S1. Growth Curves.**

**Optical density vs. time for all cultures.** Growth curves and parameters were estimated using the R package growthcurver (Sprouffske, 2018) by fitting OD measurements to the following logistic equation, where  $t$  is time,  $OD$  is the optical density, and fit parameters  $\mu$  and  $K$  represent the growth rate and carrying capacity (max OD), respectively:

$$OD_t = \frac{K}{1 + (K/OD_{t_0} - 1) \cdot e^{-\mu t}}$$

No optical density data was collected for *D. desulfuricans* and *S. loihica* which precipitated minerals during growth and could not be measured optically.



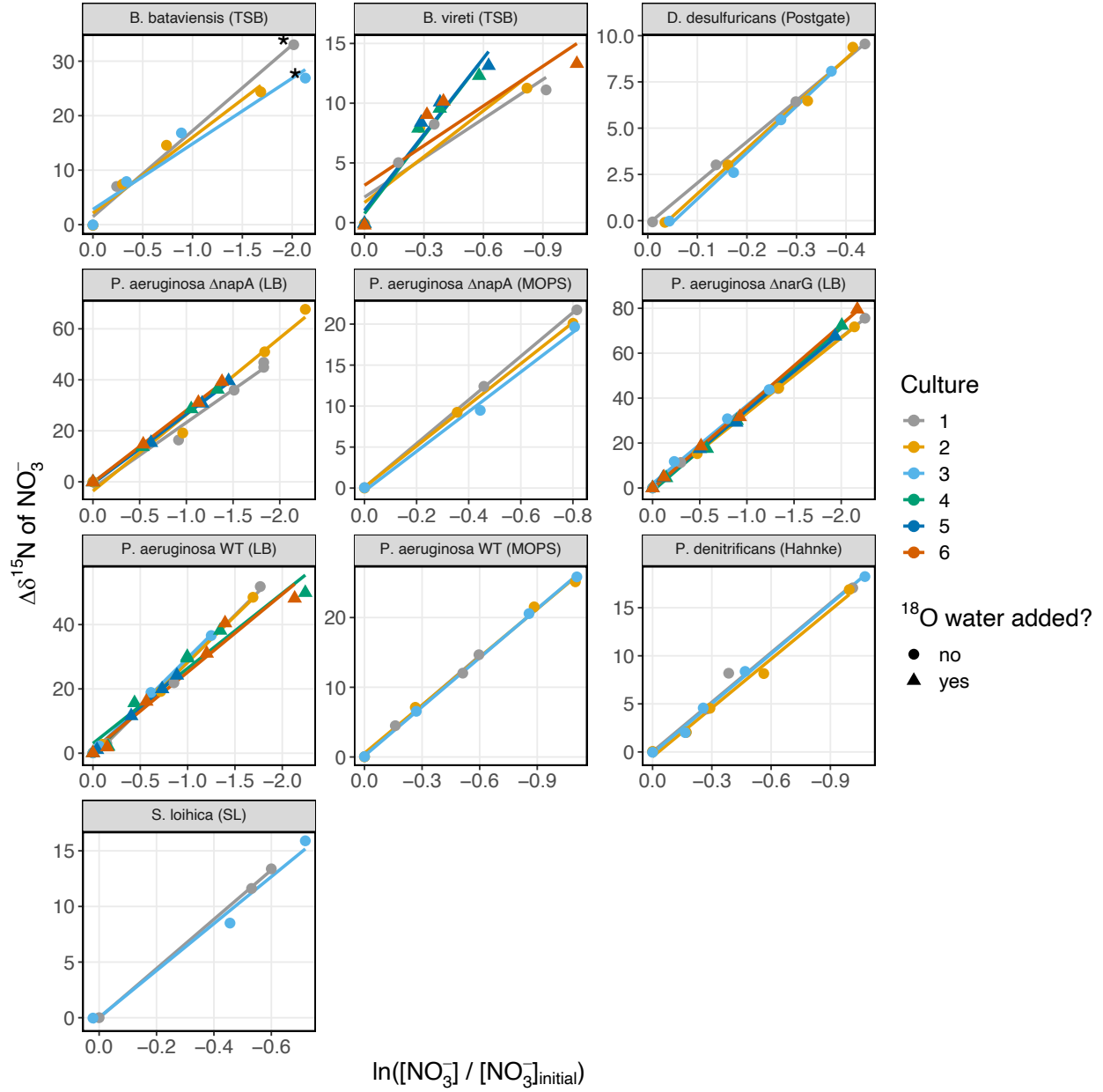


**Figure S3:  $\delta^{15}\text{N}$  vs  $\ln f$**

Change in  $\delta^{15}\text{N}$  of nitrate versus the natural log of the remaining nitrate over initial nitrate with linear regression fits to show the isotope fractionation. Triangles represent experiments where  $^{18}\text{O}$  labelled water was added. Starred (\*) datapoints indicate samples with  $> 20\text{mM}$  nitrite accumulation which were purified by ion chromatography prior to analysis (*B. bataviensis* panel).

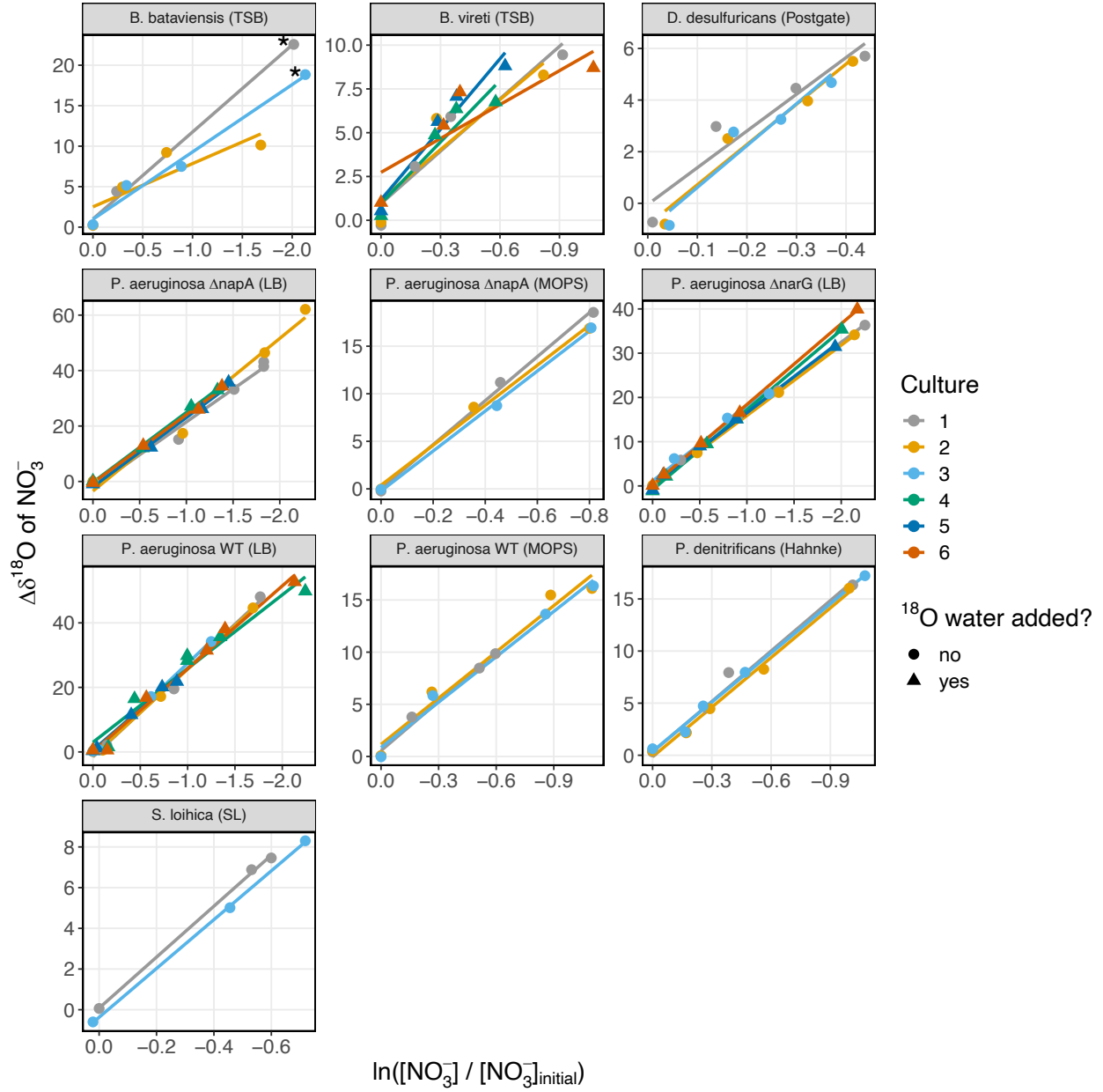


**Figure S4:  $\delta^{18}\text{O}$  vs  $\ln f$**

Change in  $\delta^{18}\text{O}$  of nitrate versus the natural log of the remaining nitrate over initial nitrate with linear regression fits to show the isotope fractionation. Triangles represent experiments where  $^{18}\text{O}$  labelled water was added. Starred (\*) datapoints indicate samples with  $> 20\text{mM}$  nitrite accumulation which were purified by ion chromatography prior to analysis (*B. bataviensis* panel).

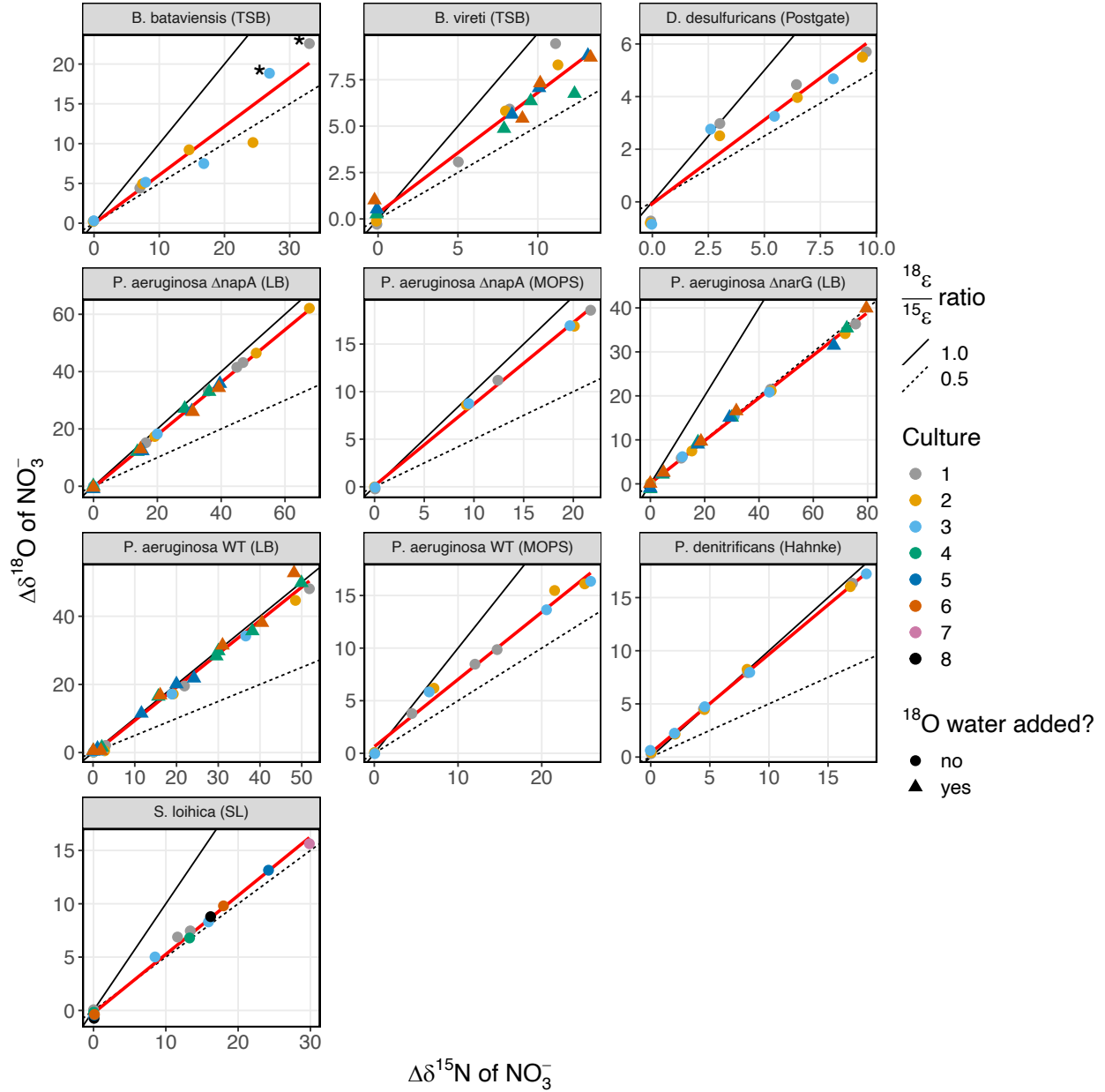


**Figure S5.  $\delta^{18}\text{O}$  vs  $\delta^{15}\text{N}$ .**

The change in  $\delta^{18}\text{O}$  versus change in  $\delta^{15}\text{N}$  for all experiments with red regression lines highlighting the  $^{18}\epsilon / ^{15}\epsilon$  coupling. Triangles represent experiments where  $^{18}\text{O}$  labelled water was added. Starred (\*) datapoints indicate samples with  $> 20\text{mM}$  nitrite accumulation which were purified by ion chromatography prior to analysis (*B. bataviensis* panel).

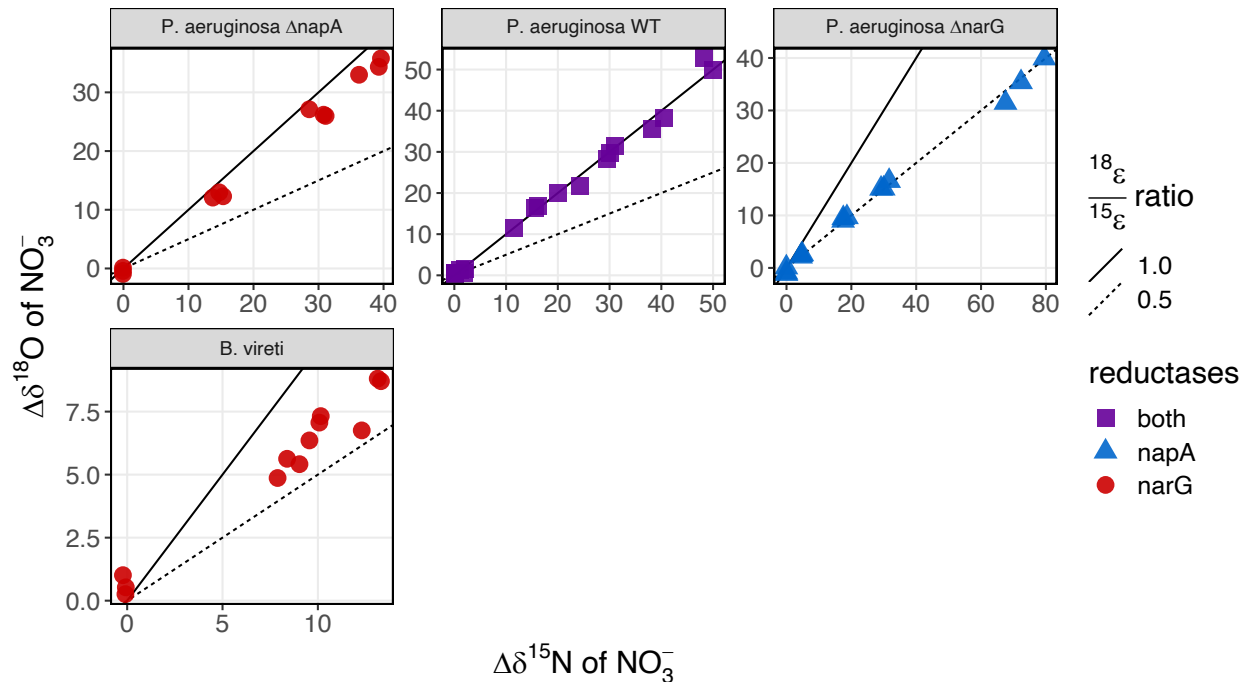


**Figure S6:  $^{18}\text{O}$  water experiments**

The change in  $\delta^{18}\text{O}$  plotted versus the change in  $\delta^{15}\text{N}$  for the PA14 mutant and wild type (WT) and *B. vireti* tracer experiments. “Nar only” corresponds to the PA  $\Delta\text{nap}$  strain, and “Nap only” corresponds to the PA  $\Delta\text{nar}$  strain. Media used in these experiments were made from  $^{18}\text{O}$  enriched water with a final  $\delta^{18}\text{O}_{\text{water}}$  of approximately 100‰. Solid lines and dashed lines indicate  $\epsilon^{18}\text{O} / \epsilon^{15}\text{N}$  of 1.0 and 0.5, respectively. All PA14 strains grown in LB.

## Supplementary Discussion: the role of nitrite

Nitrite can obscure the experimentally determined oxygen isotope fractionation and  $^{18}\epsilon / ^{15}\epsilon$  coupling associated with nitrate reduction in several ways. First, if nitrite accumulates during a nitrate reduction experiment and is not quantitatively removed prior to nitrate analysis (Granger & Sigman, 2009), it contaminates the nitrate pool and thus affects the resulting isotopic measurement with the denitrifier method (Sigman et al., 2001). Second, if nitrite is re-oxidized during a nitrate reduction experiment in significant quantities, the kinetic isotope effects of re-oxidation and introduction of water derived oxygen affects the isotopic composition of nitrate (Buchwald & Casciotti, 2010). Both of these scenarios can additionally be affected by abiotic exchange of O between nitrite and water. Below, we discuss how each of these effects would lead to systematic over / under-estimation of the  $^{18}\epsilon / ^{15}\epsilon$  coupling of nitrate reduction and how our experimental results speak to these effects.

### #1 Nitrite accumulation and incomplete nitrite removal prior to analysis (= nitrite contamination)

Because nitrate ( $\text{NO}_3^-$ ) reduction to nitrite ( $\text{NO}_2^-$ ) exhibits normal isotope effects, the residual nitrate becomes enriched in  $^{15}\text{N}$  while the resulting nitrite is depleted in  $^{15}\text{N}$ . If nitrite accumulates

in a batch culture system like ours instead of being reduced further (a closed system Rayleigh distillation, (Mariotti et al., 1981), the  $\delta^{15}\text{N}$  offset of the accumulated nitrite from the residual nitrate can be described by the equation below. The  $\delta^{15}\text{N}$  offset of nitrite from nitrate starts at  $^{15}\epsilon_{nr}$  (e.g.  $\approx -25\text{‰}$ ) and gets larger as the fraction of nitrate remaining ( $f_{NO3}$ ) decreases (to  $\approx -35\text{‰}$  with 50% nitrate remaining, to  $\approx -46\text{‰}$  with 25% nitrate remaining). An isotopic measurement of the residual nitrate pool together with some (or all) of the accumulated nitrite using the denitrifier method will thus always lead to a  $\delta^{15}\text{N}$  measurement that is lower than the  $\delta^{15}\text{N}$  of the actual nitrate pool.

$$\delta^{15}N_{NO2} - \delta^{15}N_{NO3} = \left( \delta^{15}N_{NO3_{init}} - ^{15}\epsilon_{nr} \cdot \frac{f_{NO3}}{1 - f_{NO3}} \cdot \ln f_{NO3} \right) - (\delta^{15}N_{NO3_{init}} + ^{15}\epsilon_{nr} \cdot \ln f_{NO3})$$

$$\rightarrow \delta^{15}N_{NO2} = \delta^{15}N_{NO3} - ^{15}\epsilon_{nr} \cdot \frac{1}{1 - f_{NO3}} \cdot \ln f_{NO3}$$

For  $\delta^{18}\text{O}$ , the same Rayleigh distillation takes place for the residual nitrate pool. However, the oxygen isotope composition of the accumulating nitrite pool is additionally affected by the branching isotope effect of nitrate reduction. Briefly, during nitrate reduction, the O that affects the isotopic preference of the reductase appears to be the O that is lost to water from the N-O bond cleavage. Consequently, the O isotope effect of nitrate reduction does not manifest in the resulting nitrite (only in the residual nitrate), which is commonly expressed with a so-called branching isotope effect ( $^{18}\epsilon_{br}$ ) term that is approximately equal but opposite to the reduction itself ( $\sim +25\text{‰}$ , (Casciotti et al., 2007). In a closed system Rayleigh distillation, the resulting  $\delta^{18}\text{O}$  offset of the accumulated nitrite from the residual nitrate can thus be described by:

$$\delta^{18}O_{NO2} - \delta^{18}O_{NO3} = \left( \delta^{18}O_{NO3_{init}} - ^{18}\epsilon_{nr} \cdot \frac{f_{NO3}}{1 - f_{NO3}} \cdot \ln f_{NO3} + ^{18}\epsilon_{br} \right) - (\delta^{18}O_{NO3_{init}} + ^{18}\epsilon_{nr} \cdot \ln f_{NO3})$$

$$\rightarrow \delta^{18}O_{NO2} = \delta^{18}O_{NO3} - ^{18}\epsilon_{nr} \cdot \frac{1}{1 - f_{NO3}} \cdot \ln f_{NO3} + ^{18}\epsilon_{br}$$

Importantly, this branching isotope effect also affects the isotopic analysis via the denitrifier method itself. In the denitrifier method, nitrate and nitrite are both quantitatively converted to  $\text{N}_2\text{O}$  by denitrifying bacteria lacking terminal nitrous oxide reductase (here *P. chlororaphis* f. sp. *aureofaciens* ATCC 1398). However, because sample nitrite does not undergo the first branching isotope effect from nitrate to nitrite,  $\text{N}_2\text{O}$  generated from nitrite is isotopically lighter than  $\text{N}_2\text{O}$  generated from nitrate by the same branching isotope effect of nitrate reduction (Casciotti et al., 2007). Analyzed in a nitrate reference frame, nitrite contamination effectively leads to an underestimate of nitrite  $\delta^{18}\text{O}$  by  $^{18}\epsilon_{br}$  (hereafter termed  $^{18}\epsilon_{br-dm}$  to distinguish the branching isotope effect of the denitrifier method from the branching isotope effect  $^{18}\epsilon_{br-ex}$  during batch culture experiments):

$$\rightarrow \delta^{18}O_{NO2_{dm}} = \delta^{18}O_{NO3} - ^{18}\epsilon_{nr} \cdot \frac{1}{1 - f_{NO3}} \cdot \ln f_{NO3} + ^{18}\epsilon_{br-ex} - ^{18}\epsilon_{br-dm}$$

This means that overall, if nitrite accumulates (i.e. is not consumed biologically), an isotopic measurement of the residual nitrate pool together with some (or all) of the accumulated nitrite using the denitrifier method will lead to  $\delta^{15}\text{N}$  and  $\delta^{18}\text{O}$  measurements that underestimate those of the actual nitrate pool. However, whether this leads to an overestimate or underestimate of  $^{18}\epsilon / ^{15}\epsilon$

depends on the relative magnitude of the branching isotope effect during the experiment ( $^{18}\epsilon_{\text{br-ex}}$ ) vs. during the denitrifier method ( $^{18}\epsilon_{\text{br-dm}}$ ). If  $|^{18}\epsilon_{\text{br-dm}}| = |^{18}\epsilon_{\text{br-ex}}|$ , then nitrite contamination **does not** change the actual  $^{18}\epsilon / ^{15}\epsilon$  estimates. If  $|^{18}\epsilon_{\text{br-dm}}| > |^{18}\epsilon_{\text{br-ex}}|$ , then the underestimates for  $\delta^{18}\text{O}$  become greater than the underestimates for  $\delta^{15}\text{N}$  leading to an overall **underestimate** of the actual  $^{18}\epsilon / ^{15}\epsilon$  coupling. If the reverse is the case, it would lead to an **overestimate** of  $^{18}\epsilon / ^{15}\epsilon$ . Because branching isotope effects appear to relate to the isotope effects of nitrate reduction and the organism used for the denitrifier method has larger fractionation factors and branching isotope effects than the organisms in that study that accumulate nitrite (*P. chlororaphis* has  $^{15}\epsilon_{\text{nr}}$  of  $-20.1 \pm 2.4\%$ , Granger et al., 2008); its estimated  $^{18}\epsilon_{\text{br-dm}}$  is 25 to 30%, Casciotti et al., 2007), we assume that nitrite contamination has either **no effect or leads to an underestimate** of  $^{18}\epsilon / ^{15}\epsilon$  (**scenario #1, Figure S6**). Abiotic nitrite-water exchange would amplify this effect, see section on exchange below for details.

## #2 Nitrite re-oxidation

During nitrite oxidation, whether mediated by a nitrite oxidoreductase in nitrification or reversibility in the Nar or Nap reductases, two oxygen atoms are inherited from the nitrite molecule being oxidized and the third oxygen atom is derived from water (Buchwald & Casciotti, 2010). In contrast with the N isotopes, the O isotope composition of the resulting nitrate is therefore always affected by the O isotope composition of water ( $\delta^{18}\text{O}_{\text{H}_2\text{O}}$ ). For nitrification, there is a normal kinetic isotope effect associated with water incorporation ( $^{18}\epsilon_{\text{k, H}_2\text{O}} \approx -15\%$ , (Buchwald & Casciotti, 2010), and an inverse kinetic isotope effect in both O and N associated with the nitrite oxidoreductase ( $^{18}\epsilon_{\text{k, NO}_2} = 1.3 - 8.2\%$ ,  $^{15}\epsilon_{\text{k, NO}_2} = 12.8\%$ , (Buchwald & Casciotti, 2010; Casciotti, 2009). If nitrite oxidation is quantitative, the kinetic isotope effects of the nitrite oxidoreductase have no effect, but the incorporation of the water O and fractionation associated with it always does. Although the exact isotope effects associated with nitrite oxidation by reversible Nap and Nar reductases are not yet known, it is likely that the contribution of water O in Nap/Nar reversibility would have a similar effect to water O in the nitrite oxidoreductase.

Specifically, because the kinetic isotope effect associated with water incorporation ( $^{18}\epsilon_{\text{k, H}_2\text{O}}$ ) is normal, the O derived from water during nitrite re-oxidation is always isotopically lighter than water (by  $\approx -15\%$ ). If the O isotopic composition of water and starting nitrite/nitrate are comparable, or if water is isotopically lighter than nitrite/nitrate ( $\delta^{18}\text{O}_{\text{H}_2\text{O}} \leq \delta^{18}\text{O}_{\text{nitrite}} \approx \delta^{18}\text{O}_{\text{nitrate}}$ ), nitrite re-oxidation would thus contribute isotopically lighter O and lead to an **underestimate** of the  $^{18}\epsilon / ^{15}\epsilon$  coupling of nitrate reduction (**scenario #2, Figure S6**). Only if water is significantly enriched in  $^{18}\text{O}$  ( $\delta^{18}\text{O}_{\text{H}_2\text{O}} \gg \delta^{18}\text{O}_{\text{nitrite}} \approx \delta^{18}\text{O}_{\text{nitrate}}$ ) could nitrite re-oxidation contribute isotopically heavier O and lead to an **overestimate** of the  $^{18}\epsilon / ^{15}\epsilon$  coupling of nitrate reduction (**scenario #3, Figure S6**).

In our experimental conditions with ambient water ( $\delta^{18}\text{O}_{\text{H}_2\text{O}} \approx -16\%$ ,  $^{18}\text{O}_{\text{nitrate}} \approx +22\%$ ), nitrite re-oxidation would lead to an underestimate of  $^{18}\epsilon / ^{15}\epsilon$ . In our experimental conditions with  $^{18}\text{O}$  enriched water ( $\delta^{18}\text{O}_{\text{H}_2\text{O}} \approx +100\%$ ,  $^{18}\text{O}_{\text{nitrate}} \approx +22\%$ ), nitrite re-oxidation would lead to an overestimate of the  $^{18}\epsilon / ^{15}\epsilon$  coupling.

## O exchange between nitrite and water

Nitrite can abiotically exchange O with water in a pH-dependent manner on experimentally and environmentally relevant timescales (Buchwald et al., 2012; Buchwald & Casciotti, 2010;

Casciotti et al., 2010; Grabb et al., 2017). This isotopic equilibration leads to a scrambling of the prior O isotopic signature of nitrite and instead drives it towards water-nitrite equilibrium with fractionation factor  $^{18}\epsilon_{eq} \approx 14\text{‰}$ , (Casciotti & McIlvin, 2007).

In combination with nitrite accumulation and incomplete removal prior to analysis by the denitrifier method (scenario #1 above), water-nitrite equilibration can either amplify the underestimation of the  $^{18}\epsilon / ^{15}\epsilon$  if  $\delta^{18}\text{O}_{\text{H}_2\text{O}} + 14\text{‰} < \delta^{18}\text{O}_{\text{nitrate}}$  or counteract the overestimation of the  $^{18}\epsilon / ^{15}\epsilon$  if  $\delta^{18}\text{O}_{\text{H}_2\text{O}} + 14\text{‰} > \delta^{18}\text{O}_{\text{nitrate}}$ . In our experimental conditions with ambient water ( $\delta^{18}\text{O}_{\text{H}_2\text{O}} \approx -16\text{‰}$ ,  $^{18}\text{O}_{\text{nitrate}} \approx +22\text{‰}$ ), this combination would likely lead to no effect or slightly amplifying the underestimate (**scenario #4, Figure S6**). In our experimental conditions with  $^{18}\text{O}$  enriched water, however ( $\delta^{18}\text{O}_{\text{H}_2\text{O}} \approx +100\text{‰}$ ,  $^{18}\text{O}_{\text{nitrate}} \approx +22\text{‰}$ ), this combination would lead to an **overestimate** of the  $^{18}\epsilon / ^{15}\epsilon$  coupling instead (**scenario #7, Figure S6**).

Water-nitrite equilibration in combination with nitrite re-oxidation (scenario #2 above), can further exacerbate the underestimate of the  $^{18}\epsilon / ^{15}\epsilon$  if  $\delta^{18}\text{O}_{\text{H}_2\text{O}} \ll \delta^{18}\text{O}_{\text{nitrate}}$ , counteract the underestimate of the  $^{18}\epsilon / ^{15}\epsilon$  coupling if  $\delta^{18}\text{O}_{\text{H}_2\text{O}} + 14\text{‰} > \delta^{18}\text{O}_{\text{nitrate}}$ , or lead to an overestimate of the  $^{18}\epsilon / ^{15}\epsilon$  coupling if  $\delta^{18}\text{O}_{\text{H}_2\text{O}} \gg \delta^{18}\text{O}_{\text{nitrate}}$ . In our experimental conditions with ambient water ( $\delta^{18}\text{O}_{\text{H}_2\text{O}} \approx -16\text{‰}$ ,  $^{18}\text{O}_{\text{nitrate}} \approx +22\text{‰}$ ), this combination would further **exacerbate the underestimate** of the  $^{18}\epsilon / ^{15}\epsilon$  coupling (**scenario #5, Figure S6**). In our experimental conditions with  $^{18}\text{O}$  enriched water ( $\delta^{18}\text{O}_{\text{H}_2\text{O}} \approx +100\text{‰}$ ,  $^{18}\text{O}_{\text{nitrate}} \approx +22\text{‰}$ ), this combination would instead lead to an **overestimate** of the  $^{18}\epsilon / ^{15}\epsilon$  coupling (**scenario #6, Figure S6**).

### ***Experimental results from experiments with $^{18}\text{O}$ enriched water***

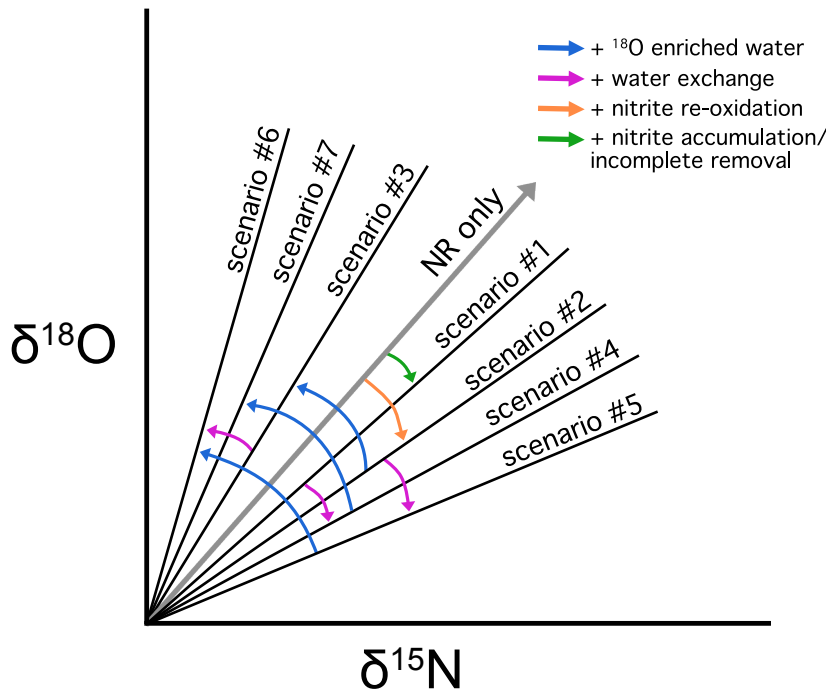
If there was significant nitrite re-oxidation, nitrite re-oxidation with water exchange, or nitrite accumulation with nitrite-water exchange occurring in our experimental conditions with  $^{18}\text{O}$  enriched water, we would expect to observe a significant shift towards higher  $^{18}\epsilon / ^{15}\epsilon$  proportionalities compared to the same experiments in ambient water. We did not observe evidence for such a shift in our experiments with  $^{18}\text{O}$  enriched water, indicating that nitrite re-oxidation and nitrite-water exchange did not play a significant role and did not obscure our experimental determination of the  $^{18}\epsilon / ^{15}\epsilon$  coupling values. However, these experiments cannot rule out that nitrite contamination, *i.e.* nitrite accumulation and incomplete removal prior to analysis (**scenario #1, Fig. S6**) could have occurred under some experimental conditions.

### ***Nitrite contamination in the *B. vireti* and *B. bataviensis* experiments***

The nitrite concentration data from the *Bacillus* strains suggests that significant amounts of nitrite built up over the course of the experiments. While sulfamic acid was used to remove the nitrite, this might have not been quantitative in all samples.

For *B. vireti*, the data points where the organisms had built up significant nitrite show lower than expected  $\delta^{15}\text{N}$  and  $\delta^{18}\text{O}$  measurements (see Fig. S3 and S4, *B. vireti* panel last data points) consistent with the predicted effects of nitrite contamination. However, the  $^{18}\epsilon / ^{15}\epsilon$  values follow a straight line (Fig. S5) suggesting that  $^{18}\epsilon$  and  $^{15}\epsilon$  are affected similarly by the nitrite contamination with little effect on the overall  $^{18}\epsilon / ^{15}\epsilon$  ratio (see discussion on nitrite contamination above).

For *B. bataviensis* on the other hand, we observed a bending of the  $^{18}\epsilon / ^{15}\epsilon$  ratio away from a straight line as nitrite accumulated (Fig. S5). This would suggest that  $^{18}\epsilon$  and  $^{15}\epsilon$  were affected differently by nitrite contamination either through differences in the branching isotope effects between *B. bataviensis* and the denitrifier organism *P. chlororaphis* (scenario #1, Fig. S6) and/or that water exchanged with the accumulated nitrite (scenario #4, Fig. S6). For this reason, we used ion chromatography for the *B. bataviensis* samples with the highest nitrite accumulation (Figure S2-S5, starred \* data points) to separate nitrite from nitrate with a fraction collector. The final isotope measurements for these samples represent purified nitrate without nitrite contamination and show  $^{18}\epsilon / ^{15}\epsilon$  values consistent with the earlier datapoints (Fig. S5, *B. bataviensis* panel). We recommend nitrate purification by fractionation collection for all samples that have excessive nitrite build-up.



**SI. Fig S6:** A schematic depicting the impact of nitrite isotope effects on  $^{18}\epsilon / ^{15}\epsilon$  values. The grey line represents an  $^{18}\epsilon / ^{15}\epsilon$  value of unidirectional fractionation via nitrate reduction (NR). This represents conditions where only nitrate reduction occurs and there is no exchange with ambient water. Arrows indicate the conditions that change the  $^{18}\epsilon / ^{15}\epsilon$  coupling in each scenario. Scenario #1 represents  $^{18}\epsilon / ^{15}\epsilon$  values where NR occurs with nitrite accumulation and incomplete nitrite removal during analysis. Scenario #2 shows the  $^{18}\epsilon / ^{15}\epsilon$  values where NR occurs in tandem with nitrite re-oxidation with low  $\delta^{18}\text{O}_{\text{water}}$ . Scenario #3 shows the impacts of NR with nitrite re-oxidation in elevated  $\delta^{18}\text{O}_{\text{water}}$ . Scenario #4 represents NR with nitrite accumulation/ incomplete removal where nitrite-water exchange has occurred. Scenario #5 shows NR with nitrite re-oxidation and nitrite-water exchange in low  $\delta^{18}\text{O}_{\text{water}}$ . Scenario #6 shows NR with nitrite re-oxidation and nitrite-water exchange in elevated  $\delta^{18}\text{O}_{\text{water}}$ . Scenario #7 shows the impacts of NR with nitrite accumulation and incomplete nitrite removal, in addition to nitrite-water exchange occurring in elevated  $\delta^{18}\text{O}_{\text{water}}$ .

## Supplementary Discussion: Data collection for Fig. 1

### Terrestrial Datasets

The data displayed in Figure 2 includes terrestrial datasets available in the literature with paired  $\delta^{15}\text{N}$  and  $\delta^{18}\text{O}$  measurements from samples collected along transects with likely the same initial nitrate source. Below are descriptions of each dataset and the relevant tables/figures in the original publications.

1. Böttcher *et al.* (1990) measured groundwater samples from different depths in wells impacted by agricultural land use. See  $\delta^{15}\text{N}$  and  $\delta^{18}\text{O}$  data in Table 1 and Figure 2 from the arable sampling sites considered by the authors to reflect the same recharge (N5, N10, N11, N12).
2. Aravena & Robertson (1998) measured samples along a groundwater flow path of septic contamination in an aquifer. See  $\delta^{15}\text{N}$  and  $\delta^{18}\text{O}$  data in Figure 5.
3. Cey *et al.* (1999) measured groundwater samples along a gradient from agricultural runoff into a riparian zone. See  $\delta^{15}\text{N}$  and  $\delta^{18}\text{O}$  data in Figure 12.
4. Mengis *et al.* (1999) measured samples from groundwater along a drainage creek. See  $\delta^{15}\text{N}$  and  $\delta^{18}\text{O}$  data in Table 1.
5. Lehmann *et al.* (2003) measured samples from a depth profile through the hypolimnion in the southern basin of Lake Lugano. See  $\delta^{15}\text{N}$  and  $\delta^{18}\text{O}$  data in Figure 3.
6. Wenk *et al.* (2014) measured samples from a depth profile through the oxic hypolimnion and the redox transition zone in the northern basin of Lake Lugano. See  $\delta^{15}\text{N}$  and  $\delta^{18}\text{O}$  data in Figure 5 (excluding the epilimnion).

### Marine Datasets

A much larger number of datasets with paired  $\delta^{15}\text{N}$  and  $\delta^{18}\text{O}$  measurements exists for marine than for terrestrial samples. The data included in Figure 2 was derived from a compilation by Fripiat *et al.* (in review) and includes data from the following publications: Bourbonnais *et al.*, 2009; K. L. Casciotti *et al.*, 2018; Karen L. Casciotti *et al.*, 2013; K.L. Casciotti & McIlvin, 2007; Dehairs *et al.*, 2015; DeVries *et al.*, 2013; DiFiore *et al.*, 2009; Gaye *et al.*, 2013; Harms *et al.*, 2019; Kemeny *et al.*, 2016; Knapp *et al.*, 2008, 2011; M. F. Lehmann *et al.*, 2005; N. Lehmann *et al.*, 2018; Marconi *et al.*, 2015; Marconi, Kopf, *et al.*, 2017; Marconi, Sigman, *et al.*, 2017; Martin & Casciotti, 2017; Pantoja *et al.*, 2002; Peng *et al.*, 2018; Rafter *et al.*, 2012, 2013; Rafter & Sigman, 2016; Daniel M. Sigman *et al.*, 2009; Smart *et al.*, 2015; Trull *et al.*, 2008; Van Oostende *et al.*, 2017; Yoshikawa *et al.*, 2018.

## References

- Aravena, R., & Robertson, W. D. (1998). Use of multiple isotope tracers to evaluate denitrification in ground water: Study of nitrate from a large-flux septic system plume. *Ground Water*, 36(6), 975–982.
- Böttcher, J., Strebel, O., Voerkelius, S., & Schmidt, H.-L. (1990). Using isotope fractionation of nitrate-nitrogen and nitrate-oxygen for evaluation of microbial denitrification in a sandy aquifer. *Journal of Hydrology*, 114(3–4), 413–424. [https://doi.org/10.1016/0022-1694\(90\)90068-9](https://doi.org/10.1016/0022-1694(90)90068-9)
- Bourbonnais, A., Lehmann, M. F., Waniek, J. J., & Schulz-Bull, D. E. (2009). Nitrate isotope anomalies reflect N<sub>2</sub> fixation in the Azores Front region (subtropical NE Atlantic). *Journal of Geophysical Research: Oceans*, 114(C3).
- Buchwald, C., & Casciotti, K. L. (2010). Oxygen isotopic fractionation and exchange during bacterial nitrite oxidation. *Limnology and Oceanography*, 55(3), 1064–1074. <https://doi.org/10.4319/lo.2010.55.3.1064>
- Buchwald, C., Santoro, A. E., McIlvin, M. R., & Casciotti, K. L. (2012). Oxygen isotopic composition of nitrate and nitrite produced by nitrifying cocultures and natural marine assemblages. *Limnology and Oceanography*, 57(5), 1361–1375. <https://doi.org/10.4319/lo.2012.57.5.1361>
- Casciotti, K. L., Forbes, M., Vedamati, J., Peters, B. D., Martin, T. S., & Mordy, C. W. (2018). Nitrous oxide cycling in the Eastern Tropical South Pacific as inferred from isotopic and isotopomeric data. *Deep Sea Research Part II: Topical Studies in Oceanography*, 156, 155–167. <https://doi.org/10.1016/j.dsr2.2018.07.014>
- Casciotti, Karen L. (2009). Inverse kinetic isotope fractionation during bacterial nitrite oxidation. *Geochimica et Cosmochimica Acta*, 73(7), 2061–2076. <https://doi.org/10.1016/j.gca.2008.12.022>
- Casciotti, Karen L., Böhlke, J. K., McIlvin, M. R., Mroczkowski, S. J., & Hannon, J. E. (2007). Oxygen Isotopes in Nitrite: Analysis, Calibration, and Equilibration. *Analytical Chemistry*, 79(6), 2427–2436. <https://doi.org/10.1021/ac061598h>
- Casciotti, Karen L., Buchwald, C., & McIlvin, M. (2013). Implications of nitrate and nitrite isotopic measurements for the mechanisms of nitrogen cycling in the Peru oxygen deficient zone. *Deep Sea Research Part I: Oceanographic Research Papers*, 80, 78–93. <https://doi.org/10.1016/j.dsr.2013.05.017>
- Casciotti, Karen L., McIlvin, M., & Buchwald, C. (2010). Oxygen isotopic exchange and fractionation during bacterial ammonia oxidation. *Limnology and Oceanography*, 55(2), 753–762. <https://doi.org/10.4319/lo.2010.55.2.0753>
- Casciotti, K.L., & McIlvin, M. R. (2007). Isotopic analyses of nitrate and nitrite from reference mixtures and application to Eastern Tropical North Pacific waters. *Marine Chemistry*, 107(2), 184–201. <https://doi.org/10.1016/j.marchem.2007.06.021>
- Cey, E. E., Rudolph, D. L., Aravena, R., & Parkin, G. (1999). Role of the riparian zone in controlling the distribution and fate of agricultural nitrogen near a small stream in southern Ontario. *Journal of Contaminant Hydrology*, 37(1–2), 45–67.
- Dehairs, F., Fripiat, F., Cavagna, A.-J., Trull, T. W., Fernandez, C., Davies, D., Roukaerts, A., Fonseca Batista, D., Planchon, F., & Elskens, M. (2015). Nitrogen cycling in the Southern Ocean Kerguelen Plateau area: Evidence for significant surface nitrification from nitrate isotopic compositions. *Biogeosciences*, 12(5), 1459–1482.

- DeVries, T., Deutsch, C., Rafter, P. A., & Primeau, F. (2013). Marine denitrification rates determined from a global 3-D inverse model. *Biogeosciences*, 10(4), 2481–2496.
- DiFiore, P. J., Sigman, D. M., & Dunbar, R. B. (2009). Upper ocean nitrogen fluxes in the Polar Antarctic Zone: Constraints from the nitrogen and oxygen isotopes of nitrate: POLAR ANTARCTIC NITRATE N AND O ISOTOPES. *Geochemistry, Geophysics, Geosystems*, 10(11), n/a-n/a. <https://doi.org/10.1029/2009GC002468>
- Gaye, B., Nagel, B., Dähnke, K., Rixen, T., & Emeis, K.-C. (2013). Evidence of parallel denitrification and nitrite oxidation in the ODZ of the Arabian Sea from paired stable isotopes of nitrate and nitrite. *Global Biogeochemical Cycles*, 27(4), 1059–1071. <https://doi.org/10.1002/2011GB004115>
- Grabb, K. C., Buchwald, C., Hansel, C. M., & Wankel, S. D. (2017). A dual nitrite isotopic investigation of chemodenitrification by mineral-associated Fe (II) and its production of nitrous oxide. *Geochimica et Cosmochimica Acta*, 196, 388–402.
- Granger, J., & Sigman, D. M. (2009). Removal of nitrite with sulfamic acid for nitrate N and O isotope analysis with the denitrifier method. *Rapid Communications in Mass Spectrometry*, 23(23), 3753–3762. <https://doi.org/10.1002/rcm.4307>
- Granger, J., Sigman, D. M., Lehmann, M. F., & Tortell, P. D. (2008). Nitrogen and oxygen isotope fractionation during dissimilatory nitrate reduction by denitrifying bacteria. *Limnology and Oceanography*, 53(6), 2533–2545. <https://doi.org/10.4319/lo.2008.53.6.2533>
- Harms, N. C., Lahajnar, N., Gaye, B., Rixen, T., Dähnke, K., Ankele, M., Schwarz-Schampera, U., & Emeis, K.-C. (2019). Nutrient distribution and nitrogen and oxygen isotopic composition of nitrate in water masses of the subtropical southern Indian Ocean. *Biogeosciences*, 16(13), 2715–2732.
- Kemeny, P. C., Weigand, M. A., Zhang, R., Carter, B. R., Karsh, K. L., Fawcett, S. E., & Sigman, D. M. (2016). Enzyme-level interconversion of nitrate and nitrite in the fall mixed layer of the Antarctic Ocean. *Global Biogeochemical Cycles*, 30(7), 1069–1085.
- Knapp, A. N., DiFiore, P. J., Deutsch, C., Sigman, D. M., & Lipschultz, F. (2008). Nitrate isotopic composition between Bermuda and Puerto Rico: Implications for N<sub>2</sub> fixation in the Atlantic Ocean. *Global Biogeochemical Cycles*, 22(3).
- Knapp, A. N., Sigman, D. M., Lipschultz, F., Kustka, A. B., & Capone, D. G. (2011). Interbasin isotopic correspondence between upper-ocean bulk DON and subsurface nitrate and its implications for marine nitrogen cycling. *Global Biogeochemical Cycles*, 25(4).
- Lehmann, M. F., Reichert, P., Bernasconi, S. M., Barbieri, A., & McKenzie, J. A. (2003). Modelling nitrogen and oxygen isotope fractionation during denitrification in a lacustrine redox-transition zone. *Geochimica et Cosmochimica Acta*, 67(14), 2529–2542. [https://doi.org/10.1016/S0016-7037\(03\)00085-1](https://doi.org/10.1016/S0016-7037(03)00085-1)
- Lehmann, M. F., Sigman, D. M., McCorkle, D. C., Brunelle, B. G., Hoffmann, S., Kienast, M., Cane, G., & Clement, J. (2005). Origin of the deep Bering Sea nitrate deficit: Constraints from the nitrogen and oxygen isotopic composition of water column nitrate and benthic nitrate fluxes. *Global Biogeochemical Cycles*, 19(4).
- Lehmann, N., Granger, J., Kienast, M., Brown, K. S., Rafter, P. A., Martínez-Méndez, G., & Mohtadi, M. (2018). Isotopic evidence for the evolution of subsurface nitrate in the Western Equatorial Pacific. *Journal of Geophysical Research: Oceans*, 123(3), 1684–1707.

- Marconi, D., Kopf, S., Rafter, P. A., & Sigman, D. M. (2017). Aerobic respiration along isopycnals leads to overestimation of the isotope effect of denitrification in the ocean water column. *Geochimica et Cosmochimica Acta*, 197, 417–432.
- Marconi, D., Sigman, D. M., Casciotti, K. L., Campbell, E. C., Alexandra Weigand, M., Fawcett, S. E., Knapp, A. N., Rafter, P. A., Ward, B. B., & Haug, G. H. (2017). Tropical dominance of N<sub>2</sub> fixation in the North Atlantic Ocean. *Global Biogeochemical Cycles*, 31(10), 1608–1623.
- Marconi, D., Weigand, M. A., Rafter, P. A., McIlvin, M. R., Forbes, M., Casciotti, K. L., & Sigman, D. M. (2015). Nitrate isotope distributions on the US GEOTRACES North Atlantic cross-basin section: Signals of polar nitrate sources and low latitude nitrogen cycling. *Marine Chemistry*, 177, 143–156.
- Mariotti, A., Germon, J. C., Hubert, P., Kaiser, P., Letolle, R., Tardieux, A., & Tardieux, P. (1981). Experimental determination of nitrogen kinetic isotope fractionation: Some principles; illustration for the denitrification and nitrification processes. *Plant and Soil*, 62(3), 413–430. <https://doi.org/10.1007/BF02374138>
- Martin, T. S., & Casciotti, K. L. (2017). Paired N and O isotopic analysis of nitrate and nitrite in the Arabian Sea oxygen deficient zone. *Deep Sea Research Part I: Oceanographic Research Papers*, 121, 121–131.
- Mengis, M., Schiff, S. L., Harris, M., English, M. C., Aravena, R., Elgood, R. J., & MacLean, A. (1999). Multiple geochemical and isotopic approaches for assessing ground water NO<sub>3</sub>-elimination in a riparian zone. *Ground Water*, 37(3), 448–457.
- Pantoja, S., Repeta, D. J., Sachs, J. P., & Sigman, D. M. (2002). Stable isotope constraints on the nitrogen cycle of the Mediterranean Sea water column. *Deep Sea Research Part I: Oceanographic Research Papers*, 49(9), 1609–1621.
- Peng, X., Fawcett, S. E., Van Oostende, N., Wolf, M. J., Marconi, D., Sigman, D. M., & Ward, B. B. (2018). Nitrogen uptake and nitrification in the subarctic North Atlantic Ocean. *Limnology and Oceanography*, 63(4), 1462–1487.
- Rafter, P. A., DiFiore, P. J., & Sigman, D. M. (2013). Coupled nitrate nitrogen and oxygen isotopes and organic matter remineralization in the Southern and Pacific Oceans: Nitrate Isotopes and Remineralization. *Journal of Geophysical Research: Oceans*, 118(10), 4781–4794. <https://doi.org/10.1002/jgrc.20316>
- Rafter, P. A., & Sigman, D. M. (2016). Spatial distribution and temporal variation of nitrate nitrogen and oxygen isotopes in the upper equatorial Pacific Ocean. *Limnology and Oceanography*, 61(1), 14–31.
- Rafter, P. A., Sigman, D. M., Charles, C. D., Kaiser, J., & Haug, G. H. (2012). Subsurface tropical Pacific nitrogen isotopic composition of nitrate: Biogeochemical signals and their transport. *Global Biogeochemical Cycles*, 26(1).
- Sigman, D. M., Casciotti, K. L., Andreani, M., Barford, C., Galanter, M., & Böhlke, J. K. (2001). A Bacterial Method for the Nitrogen Isotopic Analysis of Nitrate in Seawater and Freshwater. *Analytical Chemistry*, 73(17), 4145–4153. <https://doi.org/10.1021/ac010088e>
- Sigman, Daniel M., DiFiore, P. J., Hain, M. P., Deutsch, C., & Karl, D. M. (2009). Sinking organic matter spreads the nitrogen isotope signal of pelagic denitrification in the North Pacific. *Geophysical Research Letters*, 36(8).
- Smart, S. M., Fawcett, S. E., Thomalla, S. J., Weigand, M. A., Reason, C. J., & Sigman, D. M. (2015). Isotopic evidence for nitrification in the Antarctic winter mixed layer. *Global Biogeochemical Cycles*, 29(4), 427–445.

- Trull, T. W., Davies, D., & Casciotti, K. (2008). Insights into nutrient assimilation and export in naturally iron-fertilized waters of the Southern Ocean from nitrogen, carbon and oxygen isotopes. *Deep Sea Research Part II: Topical Studies in Oceanography*, 55(5–7), 820–840.
- Van Oostende, N., Fawcett, S. E., Marconi, D., Lueders-Dumont, J., Sabadel, A. J. M., Woodward, E. M. S., Jönsson, B. F., Sigman, D. M., & Ward, B. B. (2017). Variation of summer phytoplankton community composition and its relationship to nitrate and regenerated nitrogen assimilation across the North Atlantic Ocean. *Deep Sea Research Part I: Oceanographic Research Papers*, 121, 79–94.
- Wenk, C. B., Zopfi, J., Blees, J., Veronesi, M., Niemann, H., & Lehmann, M. F. (2014). Community N and O isotope fractionation by sulfide-dependent denitrification and anammox in a stratified lacustrine water column. *Geochimica et Cosmochimica Acta*, 125, 551–563. <https://doi.org/10.1016/j.gca.2013.10.034>
- Yoshikawa, C., Makabe, A., Matsui, Y., Nunoura, T., & Ohkouchi, N. (2018). Nitrate isotope distribution in the subarctic and subtropical North Pacific. *Geochemistry, Geophysics, Geosystems*, 19(7), 2212–2224.